Atmos. Chem. Phys. Discuss., 10, 657–710, 2010
www.atmos-chem-phys-discuss.net/10/657/2010/

Atmospheric Chemistry and Physics Discussions

This discussion paper is/has been under review for the journal Atmospheric Chemistry and Physics (ACP). Please refer to the corresponding final paper in ACP if available.

Potential contribution of semi-volatile and intermediate volatility primary organic compounds to secondary organic aerosol in the Mexico City region

A. Hodzic[1], J. L. Jimenez[2], S. Madronich[1], M. R. Canagaratna[3], P. F. DeCarlo[2,4,*], L. Kleinman[5], and J. Fast[6]

[1]National Center for Atmospheric Research, Boulder, CO, USA
[2]Dept. of Chemistry and Biochemistry, and CIRES, Univ. of Colorado, Boulder, CO, USA
[3]Aerodyne Research, Billerica, MA, USA
[4]Dept. of Atmospheric and Oceanic Science, Univ. of Colorado, Boulder, CO, USA
[5]Brookhaven National Laboratory, Upton, New York, USA
[6]Pacific Northwest National Laboratory, Richland, WA, USA
[*]now at: Laboratory of Atmospheric Chemistry, Paul Scherrer Institut, Villigen, Switzerland

Received: 10 December 2009 – Accepted: 21 December 2009 – Published: 14 January 2010

Correspondence to: A. Hodzic (alma@ucar.edu)

Published by Copernicus Publications on behalf of the European Geosciences Union.

Abstract

It has been established that observed local and regional levels of secondary organic aerosols (SOA) in polluted areas cannot be explained by the oxidation and partitioning of anthropogenic and biogenic VOC precursors, at least using current mechanisms and parameterizations. In this study, the 3-D regional air quality model CHIMERE is applied to quantify the contribution to SOA formation of recently identified semi-volatile and intermediate volatility organic vapors (S/IVOC) in and around Mexico City for the MILAGRO field experiment during March 2006. The model has been updated to include explicitly the volatility distribution of primary organic aerosols (POA), their gas-particle partitioning and the gas-phase oxidation of the vapors. Two recently proposed parameterizations, those of Robinson et al. (2007) ("ROB") and Grieshop et al. (2009) ("GRI") are compared and evaluated against surface and aircraft measurements. The 3-D model results are assessed by comparing with the concentrations of OA components from Positive Matrix Factorization of Aerosol Mass Spectrometer (AMS) data, and for the first time also with oxygen-to-carbon ratios derived from high-resolution AMS measurements.

The results show a substantial enhancement in predicted SOA concentrations (3–6 times) with respect to the previously published base case without S/IVOCs (Hodzic et al., 2009), both within and downwind of the city leading to much reduced discrepancies with the total OA measurements. The predicted anthropogenic POA levels are found to agree within 20% with the observed HOA concentrations for both the ROB and GRI simulations, consistent with the interpretation of the emissions inventory by previous studies. The impact of biomass burning POA within the city is underestimated in comparison to the AMS BBOA, presumably due to insufficient nighttime smoldering emissions. Model improvements in OA predictions are associated with the better-captured SOA magnitude and diurnal variability. The predicted production from anthropogenic and biomass burning S/IVOC represents 40–60% of the total SOA at the surface during the day and is somewhat larger than that from aromatics, especially at the T1 site at

the edge of the city. The SOA production from the continued multi-generation S/IVOC oxidation products continues actively downwind. Similar to aircraft observations, the predicted OA/ΔCO ratio for the ROB case increases from 20–30 $\mu g\,sm^{-3}\,ppm^{-1}$ up to 60–70 $\mu g\,sm^{-3}\,ppm^{-1}$ between a fresh and 1-day aged air mass, while the GRI case produces a 30–40% higher OA growth than observed. The predicted average O/C ratio of total OA for the ROB case is 0.16 at T0, substantially below observed value of 0.5. A much better agreement for O/C ratios and temporal variability (R^2=0.63) is achieved with the updated GRI treatment. Both treatments show a deficiency in regard to POA evolution with a tendency to over-evaporate POA upon dilution of the urban plume suggesting that atmospheric HOA may be less volatile than assumed in these parameterizations. This study highlights the important potential role of S/IVOC chemistry in the SOA budget in this region, and highlights the need for improvements in current parameterizations. We note that our simulations did not include other proposed pathways of SOA formation such as formation from very volatile species like glyoxal, which can also contribute SOA mass and especially increase the O/C ratio.

1 Introduction

Organic aerosols (OA) are currently one of the most active areas of research in atmospheric chemistry and air quality. Composed of both directly emitted primary organic particles (POA) and photochemically produced secondary organic matter (SOA), they have been identified as one of the two largest constituents of submicron aerosols throughout the world, with similar concentrations as sulfate (e.g., Murphy et al., 2006; Zhang et al., 2007). Despite their abundance in the troposphere and recognized effects on climate and human health, OA emissions, ageing, and properties remain poorly understood, and as a result, poorly represented in chemical-transport models (Kanakidou et al., 2005; Hallquist et al., 2009; de Gouw and Jimenez, 2010). Biogenic SOA levels formed in clean regions appear to be well represented overall by "traditional" SOA models (e.g., Tunved et al., 2006; Hodzic et al., 2009; Chen et al., 2009; Slowik et al., 2009).

In contrast, many studies have reported that observed levels of SOA in polluted regions at both local and regional scales cannot be explained by current modeling assumptions and from the oxidation of known VOC gaseous precursors ("V-SOA", following the terminology introduced by Tsimpidi et al., 2009) (e.g., Heald et al., 2005; de Gouw et al., 2005; Volkamer et al., 2006; Pun and Seigneur, 2007; Simpson et al., 2007; Hodzic et al., 2009; Tsimpidi et al., 2009). Model discrepancies can be substantial for short oxidation times but have been found to increase downwind of source regions (e.g., Heald et al., 2005; Volkamer et al., 2006), which consequently affect the ability of models to predict aerosol regional concentrations and radiative forcing. The most commonly used traditional semi-empirical V-SOA formation approach (Odum et al., 1996) considers only the early generation oxidation of gaseous VOC precursors into two non-reactive semi-volatile products that are partitioned between gas and aerosol phases depending on temperature and OA mass concentration. Although activity coefficients are included in this formulation, they are typically set to 1 due to lack of constraints on their values. This approach does not reflect the full spectrum of potential SOA precursors, or the complexity of the OA and VOC chemical aging (Robinson et al., 2007; Jimenez et al., 2010).

In the past few years, evidence for new precursors and pathways of SOA formation has been identified. In particular, the semi-volatile character of primary organic aerosols (POA) suggested by Robinson et al. (2007) has been the focus of much recent attention. Traditionally, POA that are directly emitted into the atmosphere from various combustion sources (e.g. vehicle exhaust, biomass burning, etc.) have been modeled as hydrophobic non-volatile compounds that remain in the particulate phase throughout their lifetime, with their conversion to hydrophilic material being sometimes treated as a first-order process with a specified timescale of ∼1 day. Recent studies (Lipsky and Robinson, 2006; Robinson et al., 2007; Huffman et al., 2008, 2009a,b; Sage et al., 2008; Grieshop et al., 2009) have shown that these species should be treated as semi-volatile compounds (SVOC) that can evaporate from the particulate phase, react in the gas-phase, and repartition as SOA. Following Tsimpidi et al. (2009), we will refer to

SOA formed from SVOC as "S-SOA". In addition, intermediate volatility species (IVOC) with volatility just above the POA and SVOC species have traditionally been ignored in SOA modeling and are also typically neglected in VOC emission inventories. They are composed of species such as long-chain hydrocarbons with more than 20 C atoms, and can undergo multiple oxidation steps leading to a large amount of lower volatility precursors that are likely to partition to the aerosol phase downwind of source regions. We will refer to SOA formed from IVOC as "I-SOA", and to the combination of S-SOA plus I-SOA as "SI-SOA". The amount of SI-SOA is expected to be substantial although the amounts and chemistry of these species remain poorly characterized and these compounds have only rarely been measured (Fraser et al., 1998).

One of the key uncertainties, in addition to the chemical properties of S/IVOC vapors, concerns the treatment of the POA emissions, i.e., whether the POA in the emissions inventory is assumed to be the aerosol fraction before or after the evaporation of SVOC has occurred (Shrivastava et al., 2008; Murphy and Pandis, 2009). Air quality modeling studies based on traditional emission inventories (before evaporation of POA) have shown a modest increase in total predicted OA (from SI-SOA) in comparison to the traditional non-volatile POA approach, when the POA in the inventory is assumed to be the amount *before* evaporation of SVOC has taken place (Robinson et al., 2007; Shrivastava et al., 2008). Shrivastava et al. (2008) even reported a slightly decreased agreement between modeled and observed total OA concentrations throughout the continental US because of the evaporation of a large fraction of the POA mass. Although modest changes were obtained in predicted total OA concentrations, the fraction of oxidized OA (SOA) was substantially increased and the regional distribution of the SOA/OA ratio was more consistent with observations. More recently, Tsimpidi et al. (2009) have suggested that in the center of Mexico City SI-SOA contribute several $\mu g/m^3$ during the afternoon. Unlike Shrivastava et al. (2008), these authors assumed, based on comparisons with observations when using non-volatile POA, that the POA reported in the Mexico City Metropolitan Area (MCMA) emission inventory was the remaining aerosol fraction *after* evaporation of associated

semi-volatile vapors. They determined the SVOC emissions by multiplying POA emissions by a factor of 3, and IVOC emissions by multiplying POA+SVOC by a factor of 1.5, as specified by Robinson et al. (2007). A box model study using data from the same campaign (MCMA-2003) (Dzepina et al., 2009) has reported a larger fraction of total SOA from SI-SOA during a stagnant day in which the local emissions underwent photochemistry for several hours with limited transport. By applying thermodynamic equilibrium with the parameters specified by Robinson et al. (2007) and the measured HOA concentrations, Dzepina et al. (2009) derived an amount of S/IVOC very similar to that of Tsimpidi et al., and achieved a much better agreement with observations during the morning and early afternoon hours in Mexico City and suggested that primary SI-SOA accounts for ~55% of the observed SOA mass (~twice higher SI-SOA than V-SOA). The improved agreement between observed and predicted SOA when including SI-SOA in both studies also suggested that the POA emissions inventory in Mexico City does not include SVOC that evaporate after POA emission.

In addition to anthropogenic emissions (e.g. from diesel exhaust), a large fraction of POA emitted from biomass burning should also be considered as semi-volatile, as demonstrated by recent thermodenuder experiments (e.g., Grieshop et al., 2009; Huffman et al., 2009a,b). These SVOC should be oxidized quickly in the gas-phase, which is consistent with field studies that have observed production and/or oxidation of organic particles emitted from biomass burning (BB) (Reid et al., 2005; Capes et al., 2008; Yokelson et al., 2009). Grieshop et al. (2009) also showed that the SOA formed from BB woodstove emissions in their chamber could not be explained by V-SOA from the measured precursors (monoterpenes and aromatics) and proposed that SI-SOA represents most of the SOA formation potential from BB smoke. The initially proposed volatility distribution and aging mechanism of semi-volatile vapors (Robinson et al., 2007) has been recently updated based on comparisons of simulations with chamber experiments (Grieshop et al., 2009). Fire emissions are no longer assumed to contribute substantial IVOC in this updated approach. The lack of strong measurement-based constraints in the current treatment of POA emissions and chemistry, especially

at long aging times beyond those than can be captured in smog chambers, could lead to substantial errors in predicted concentrations and spatial distributions of both POA and SOA, and therefore deserve further evaluation.

The overall objective of the present study is to assess the potential importance of SI-SOA in the highly polluted environment of Mexico City. Specific objectives include:

1. quantifying the contribution of SI-SOA within and downwind from Mexico City and downwind outside of the city on much larger temporal and spatial scales than assessed by Dzepina et al. (2009) and Tsimpidi et al. (2009),
2. quantifying SOA production associated specifically with biomass burning activity, and
3. evaluating the model sensitivity to the S/IVOC parameterization by comparing two approaches, that of Robinson et al. (2007) and the recently revised parameterization of Grieshop et al. (2009).

We use SOA predictions from the meso-scale chemistry transport model CHIMERE in combination with measurements by the Aerosol Mass Spectrometers (AMS) from the MILAGRO 2006 field project, which were analyzed by the Positive Matrix Factorization evaluation toolkit (PMF, Ulbrich et al., 2009) to determine the contribution of different OA components. In addition to surrogate SOA concentrations, OA/ΔCO ratios (where ΔCO is the CO concentration above the regional background), and O/C ratios will be used to evaluate the model. Comparisons are performed at the surface at two locations (urban T0 and suburban T1 sites) as well as over the city and its outflow along the G-1 and C-130 aircraft flight tracks (Kleinman et al., 2008; DeCarlo et al., 2008). Mexico City is a particularly suitable region for investigating SOA formation processes because of its highly active photochemistry and large amount of available SOA precursors. POA average levels are close to 7 $\mu g/m^3$ (Aiken et al., 2009a) and are expected to be associated with a large amount of primary S/IVOC vapors.

Several aspects of OA formation in Mexico City have already been addressed in recent studies which have shown that the emissions of POA from both anthropogenic

activities and biomass burning are reasonably represented in the emission inventories and models, with perhaps some underprediction of the urban POA, and mixed results for the BB POA with overprediction downwind of some large fires but underprediction in the urban area in the early morning (e.g., Fast et al., 2009; Hodzic et al., 2009; Zavala et al., 2009). A better prediction of the temporal trend of BBOA was achieved when the emissions profile took into account the emissions during the late evening into the shallow nighttime boundary layer (Aiken et al., 2009b). The fair agreement between modeled and observed POA concentrations reported by Fast et al. (2009), Hodzic et al. (2009), and Tsimpidi et al. (2009) confirms that SVOC are unaccounted for in the POA emissions in Mexico City (i.e., that the inventory is consistent with the POA present after SVOC evaporation). Chemical analyses of submicron aerosols have revealed an active production of oxygenated organic species (OOA) within the city and their continuous production in the outflow region (e.g., Volkamer et al., 2006; DeCarlo et al., 2008; Kleinman et al., 2008; Aiken et al., 2008, 2009a,b; Herndon et al., 2008). V-SOA showed once again its limitations in the context of Mexico City (Hodzic et al., 2009), where consistently with previous studies (Volkamer et al., 2006; Dzepina et al., 2009) it failed to reproduce the observed amounts of SOA, including their production rate in the late morning, aging during the afternoon hours, and evolving background concentrations. Hodzic et al. (2009) estimated that the model underpredicted SOA mass by more than 20 Tons during the afternoon peak over the Mexico City Metropolitan Area (MCMA).

Previous studies of SI-SOA in Mexico City have focused on SOA production within the Mexico City basin during a short period of time (Dzepina et al., 2009; Tsimpidi et al., 2009) (15 h and 4 days, respectively). Dzepina et al. (2009) also performed a 3-day box-model aging simulation that suggested that SI-SOA could increase substantially in the outflow from Mexico City. However the spatially and temporally limited framework of the previous studies did not allow investigating the significance of SI-SOA over regional scales and the multi-day processing of S/IVOC in the Mexico City plume in a 3-D context. Modeling results suggest strongly that the transport of OA from the re-

gional scale is a substantial contributor to the observed SOA levels within Mexico City. Tsimpidi et al. (2009) assumed this SOA background to be between 3 and 7 $\mu g/m^3$ at the boundaries of their $\sim 150 \times 150\ km^2$ model domain to achieve a better agreement with observations. Hodzic et al. (2009) showed that the regional background is partially due to biogenic SOA ($\sim 1.5\ \mu g/m^3$) advected from the coastal mountain ranges. Regional POA emissions associated with surrounding populated areas (e.g. Cuernavaca, Puebla, Toluca) and biomass burning are also important and can contribute substantial amounts of S/IVOC vapors that, as they age, partition to the aerosol. Hodzic et al. (2009) reported that the V-SOA formed from biomass burning emissions with a traditional SOA module was very small. However it is likely that S-SOA from biomass burning may be the dominant source of SOA from these emissions (Grieshop et al., 2009) and may also contribute to the regional background. These unanswered questions provide motivation for reevaluating the significance of this formation process in a regional context over a two week time period.

The paper is organized as follows: in Sect. 2, the CHIMERE model configuration and the updates to include S/IVOCs are presented; in Sect. 3, model predictions of secondary OA presented are assessed against OA measurements both within the city and in the outflow region. The contribution of anthropogenic and biomass burning SI-SOA is quantified and compared to the traditional V-SOA formation pathway. Section 4 summarizes the conclusions of this study.

2 Model formulation and experiment design

For this study, the CHIMERE model is run from 11 to 31 March 2006 over the Mexico City region at both regional and urban scales using the same configuration and the same forcing (i.e. meteorology, emissions, boundary and initial conditions) as for our previous study presented by Hodzic et al. (2009). A detailed description of the model formulation and the aerosol treatment was given by Hodzic et al. (2009) and Bessagnet et al. (2009). Here, we only report modifications that were specifically implemented

to the organic aerosol module (i.e. dynamic POA partitioning and oxidation) for the purpose of the present study.

2.1 Modeling the SOA formation from primary S/IVOCs

To examine the importance of SI-SOA formation, we implemented within the CHIMERE model an explicit treatment of emissions, gas-particle partitioning and gas-phase oxidation of primary organic aerosols as suggested by Robinson et al. (2007). The previous approach in which POA was considered inert and non-volatile has been replaced by a dynamic treatment in which POA material can evaporate, oxidize and re-condense over time to form S-SOA, and where IVOC are emitted in an amount proportional to the POA.

The first step was to determine the amount of semi-volatile and intermediate volatility vapors that are co-emitted with the modeled particulate POA. Following Robinson et al. (2007), this was achieved by assigning a volatility distribution of POA concentrations. S/IVOCs are distributed according to their volatility into nine surrogate species (with the six of lower volatility referred to as SVOC and the three of higher volatility as IVOC; see Table 1) that partition between the gas and particle phases according to absorption into the total OA (with activity coefficient of 1 in all cases) under thermodynamic equilibrium (Pankow et al., 1994; Donahue et al., 2006).

Per the discussion above and similar to Dzepina et al. (2009) and Tsimpidi et al. (2009), we assume here that POA reported in the emission inventories, and therefore the modeled POA concentrations, correspond to the aerosol mass after evaporation of semi-volatile compounds. Therefore, this evaporated mass was added to the model in order to achieve the equilibrium with the emitted POA. According to Donahue et al. (2006) the fraction ($X_{\mathrm{aero},i}$) of particulate organic mass in equilibrium with S/IVOC is given by:

$$X_{\mathrm{aero},i} = \frac{f_i}{1 + C_i^* / C_{\mathrm{OM}}}$$

where f_i is the mass fraction of species i in the traditionally defined POA emissions, C_i^* is the effective saturation concentration of species i, C_{OM} is the mass concentration of the absorbing organic phase, and i is the number of components in the emissions (the number of lumped species). The Clausius-Clapeyron equation is used to account for changes in C_i^* with temperature with the enthalpies of vaporization estimated for each surrogate species by Robinson et al. (2007). Following Tsimpidi et al. (2009), we assumed that approximately one third of the total emitted urban POA mass is in the aerosol phase under average ambient conditions found in Mexico-City (average OA concentration of 20 $\mu g/m^3$). Based on this assumption, total SVOC emissions were determined by multiplying the POA emission fluxes by a factor of 3. In addition to SVOC, an additional mass has been added to $IVOC_7$, $IVOC_8$ and $IVOC_9$. Following Robinson et al. (2007) this mass was assumed to be 1.5 times the mass reported in POA emissions. This ratio of total IVOC to POA was experimentally determined, and it ranges from 1.5 to 3.0 for diesel engine emissions. Here we consider the conservative value of 1.5 for all emissions. Emission factors applied to each S/IVOC species are summarized in Table 1. Note that for ~10 $\mu g/m^3$ of ambient POA, the total amount of organic material (POA+SVOC+IVOC) calculated directly with the Robinson parameters is about ~80 $\mu g/m^3$ at 20 °C (Table SI-3 of Dzepina et al., 2009). The extra amount of material is a small fraction of the total organic gas+particle material in Mexico City, and is consistent with overall constraints from OH reactivity and integral FTIR stretches measured during MCMA-2003 (Heald et al., 2008; Sheehy et al., 2008; Dzepina et al., 2009), but is poorly constrained.

All POA surface anthropogenic sources (e.g. traffic) as well as biomass burning emissions were considered as semi-volatile. POA emissions associated with elevated industrial sources (i.e. point sources) were not considered as semi-volatile in this study because their volatility distribution was not available. Contribution of point sources is relatively small in the MCMA region except for the Tula refinery complex located 45 km north of the Mexico City and the flights performed over the site have not detected significant organic aerosol emissions (in contrast to SO_2 for example, DeCarlo et al.,

2008). Primary emissions and secondary trace gases and particulates were occasionally transported over the T0 and T1 sites during periods of northwesterly near-surface winds (de Foy et al., 2009).

The second modeling step consists in adding the photochemistry of S/IVOC species and their partitioning into the aerosol phase. Gas-phase oxidation by OH of all of the nine S/IVOC is assigned a rate constant of 4×10^{-11} cm^3 $molec^{-1}$ s^{-1} (as in the Robinson et al. approach)

$$S/IVOC_{i+1}^{gas} \xrightarrow[+OH]{} S/IVOC_i^{gas}$$

Each reaction is assumed to reduce the volatility of the oxidized S/IVOCs by one order of magnitude (i.e. C^* is divided by a factor of 10), with a small net increase in mass (7.5%) to account for added oxygen. Oxidized semi-volatile products from this reaction can partition to the OA phase to form SOA. The more the S/IVOC molecules become oxidized, the more likely they are to be in the aerosol phase. A continuous drop in volatility of the gas-phase material upon oxidation will result in an efficient partitioning to the aerosol phase of all the material, given sufficient time for oxidation. This may eventually lead to much higher net production of SOA downwind of the urban center (Dzepina et al., 2009).

In addition to the original parameterization of Robinson et al. (2007), here we also consider the updated version as described in Grieshop et al. (2009). Several updates have been considered compared to the original Robinson's approach, including:

1. No biomass burning emissions of IVOC are considered;

2. Each oxidation reaction is assumed to reduce the volatility of the oxidized S/IVOC vapors by two orders of magnitude (i.e. C^* drops by 100), and a larger net increase in mass of 40% is assumed to account for the addition of oxygen. The addition of oxygen was parameterized based on comparison with laboratory measurements, although it is not clear mechanistically how so much oxygen could be added in a single reaction step.

3. The OH reaction rate constants, enthalpies of vaporization, and molecular weights of the surrogate species have also been updated (Table 1).

2.2 Model application

For this study, two model simulations were carried out in order to calculate SI-SOA. The "ROB" simulation implements the parameterization of Robinson et al. (2007) in addition to V-SOA formation from anthropogenic, biomass burning and biogenic sources. The "GRI" simulation investigates the sensitivity of the SOA formation to changes in the assumptions following the updated parameterization of Grieshop et al. (2009) as described in Table 1. These two simulations are also compared to the OA simulation from Hodzic et al. (2009) that is based on the traditional SOA approach in which POA are considered as inert species. In this traditional simulation (referred as "REF" here, and as "BIO-T" by Hodzic et al., 2009) SOA is formed from both anthropogenic and biogenic VOC precursors.

For comparison with measurements, the simulated parameters are spatially and temporally interpolated to the location of the measurement sites. The ground measurements are compared with the model's lowest level ($\Delta z \sim 25$ m). It should be noted that measured and predicted concentrations of all species are reported under ambient conditions of pressure and temperature unless indicated otherwise.

3 Results and discussion

In this section we examine the performance of the model in simulating POA and SOA in and near Mexico City. Predictions of SI-SOA (ROB and GRI simulations) are presented and evaluated against the highly time-resolved AMS measurements obtained at the surface within the city (T0 and T1 sites, Sect. 3.2), as well as over the city and in the outflow region aboard the G-1 and C-130 aircraft (Sect. 3.4). The model evaluation is limited to changes in organic species because CHIMERE predictions of meteorological variables, major gaseous pollutants, and primary and secondary organic aerosols using the traditional SOA treatment (i.e. REF simulation) has already been evaluated for March 2006. Simulated submicron OA fraction including the first four and half model size bins (from 0.04 to 1.0 μm) is used for comparison with the AMS/PMF-derived components: hydrocarbon-like organic aerosol (HOA), biomass burning organic aerosols (BBOA), and total oxygenated organic aerosol (OOA) (e.g., Aiken et al., 2009a). The modeled POA from anthropogenic (biomass burning) sources is compared with HOA (BBOA), respectively, while predicted SOA is assessed against OOA. A more detailed description on AMS apportionment using PMF analysis can be found in Ulbrich et al. (2009).

3.1 Predicted OA concentrations in and around Mexico City

Figure 1 shows the spatial distribution of average TOA and SOA surface concentrations during 15–31 March 2006 as predicted by two S/IVOC (ROB and GRI) simulations and the traditional simulation. Predicted TOA mean concentrations feature similar spatial distribution in all three simulations with highest values associated with the Mexico City basin and surrounding smaller cities. Substantial differences are however obtained in terms of absolute TOA values. The GRI simulation predicts 60% higher peak TOA concentrations ($\sim$22 μg/m^3) over Mexico City in comparison to the traditional simulation (<14 μg/m^3), while ROB predicts a more moderate increase of about 20% ($\sim$18 μg/m^3). Background concentrations are also increased by a factor of 2–3

in the ROB and GRI simulations with respect to the REF simulation. The increase in predicted TOA levels by non-traditional simulations can be explained by a strong enhancement in the SOA production both near the emissions centers and in the outflow regions to the north and south of Mexico City basin as illustrated in Fig. 1b.

Indeed, SVOC and IVOC vapors are co-emitted in equilibrium with POA mainly in the city center and are progressively transported from the city to areas located downwind. During their transport, semi-volatile vapors undergo several oxidation steps, which tend to increase their ability to partition to the aerosol phase as they age. Regional emissions of POA associated with smaller cities and the occurrence of fires also contribute to emissions of fresh S/IVOCs. This combination of local and regional emissions of semi-volatile vapors and their chemical processing leads to an increase in average SOA levels throughout the domain.

The GRI simulation features the strongest SOA production with average concentrations ranging from 12 to 16 $\mu g/m^3$ inside Mexico City, which is 3–5 times higher than those predicted with the REF model. Enhancement in the regional SOA concentrations is also seen and it is a result of the photochemical aging of the SVOC and IVOC vapors that have the potential to continuously produce SOA in the outflow region, and as some of the air advected away from Mexico City can be recirculated to the region (Emmons et al., 2010). Predicted SOA levels from the GRI simulation vary from 8 to 10 $\mu g/m^3$ in the outflow region northeast of the basin, and 6 $\mu g/m^3$ in the background areas, which is substantially higher than those predicted by the REF simulation. The increase in SOA production appears to be more moderate in the ROB simulation with SOA levels close to 8 $\mu g/m^3$ in the near field, 6 $\mu g/m^3$ in the outflow region and ~3 $\mu g/m^3$ at remote locations. This difference of 30–50% in the predicted SOA levels inside the city is related to the differences in the treatment of the chemistry of S/IVOC vapors and will be further discussed in the next section.

Including the chemistry and partitioning of semi-volatile primary organic vapors leads to substantially higher and likely more realistic predictions of SOA concentrations in comparison to the traditional simulation (Hodzic et al., 2009). Predicted SOA now rep-

resents a much larger fraction (40–60%) of the total OA, which is more consistent with the observed values reported during the campaign (e.g., Aiken et al., 2009a; DeCarlo et al., 2009; Herndon et al., 2008) that are described in more detail next.

3.2 Evaluation of predicted OA within the city basin

3.2.1 Primary organic aerosols

In both non-traditional model simulations (ROB and GRI) the emitted POA is considered as a semi-volatile species. Therefore, POA can evaporate from the particle and undergo further chemical processing in the gas phase leading to production of lower volatility organic oxygenated vapors that are likely to re-condense and form SI-SOA. This dynamic treatment of POA can have major consequences on the predicted amount of POA and its effects need to be examined first.

Figures 2 and 3 compare the time series of observed primary organic aerosols from anthropogenic sources (HOA) and biomass burning (BBOA) with the corresponding modeled primary species at the T0 and T1 sites, respectively. At T0, the model reproduces fairly well the magnitude and the diurnal variations of the observed HOA for both ROB and GRI simulations (Fig. 2a) as suggested by a relatively low bias (<20%) and correlation coefficients greater than 0.5. Observed and simulated peak concentrations occur in the early morning due to traffic emissions. The peak value is reasonably well captured by the model on most days apart from a factor of two under prediction on 29 and 30 March. As also found by Hodzic et al. (2009) the simulated HOA is frequently overpredicted during nighttime (e.g. 16 March) as a result of a too shallow boundary layer and underpredicted vertical mixing in the city overnight. This overprediction can clearly be seen on the average diurnal profiles between 20:00 LT and 02:00 LT. Small differences exist between the ROB and GRI predictions, with a slightly higher modeled HOA for the GRI simulation (~5% for the average concentration), which is consistent with the fact that a larger total organic mass is available for their partitioning (Dzepina et al., 2009). The model skill in reproducing HOA has not been deteriorated or con-

siderably changed by the introduction of the dynamic partitioning of primary organic species as shown in Fig. 2, indicating that the treatment of anthropogenic emissions in the model is reasonable in the near field. POA concentrations predicted in the ROB and GRI simulations are lower than the REF model by 1 to 2 $\mu g/m^3$ through the day, suggesting that the amount of primary organic species initially emitted is slightly underpredicted, or that their volatility may be a bit too high in the model.

At the T1 site at the edge of the city (Fig. 3a), discrepancies between observed and predicted HOA concentrations are larger both in terms of magnitude and the temporal variability as already found for the traditional simulation (Hodzic et al., 2009). The model simulations show a slight overprediction (<15%) which is mainly caused by a factor of 2–3 overprediction of nighttime values as suggested by the comparison of diurnal profiles. Although the occurrence and the magnitude of the morning HOA peak associated with the traffic emissions is well captured, the correlation coefficient stays low for both non-traditional simulations (~0.3) due to nighttime inconsistencies. As for T0, the dynamic treatment of primary organic species and assumptions made for their emissions allow reasonable prediction of the anthropogenic HOA.

The predicted BBOA shows larger discrepancies with the observations. At T0 (Fig. 2b), BBOA is present throughout the period of interest (average concentration of 1.54 $\mu g/m^3$), with however higher concentrations from 15–24 March and occurrence of three large fire events on 18, 20 and 21 March characterized by peak values in the range 10–25 $\mu g/m^3$. Both simulations generally underpredict the amount of smoke POA reaching the T0 site. While the models capture the afternoon increase in BBOA concentrations, they fail to reproduce the early morning (~06:00 LT) peaks that occurred on the 18 and 21 March in a very shallow boundary layer. As already discussed in Hodzic et al. (2009), reproducing the nighttime concentrations of pollutants is very challenging as pollutant dispersion is highly sensitive to small errors in boundary layer mixing and near-surface winds. Although the gap between the model and observations seems large (here ~3 $\mu g/m^3$), it corresponds to relatively small errors in terms of emitted mass of smoke. The smoldering regime in the fire lifecycle that usually occurs

in the early morning and can produce large quantities of smoke is not well depicted in the emissions. In our simulations, diurnal profiles with maximum emissions in the early afternoon (12:00–16:00 LT) are applied. Aiken et al. (2009b) achieved a better correlation between the BBOA at T0 and model prediction by using a modified emissions profile which includes smoldering emissions into the late evening and night. It is also likely that some fire sources are missing from the biomass burning emission inventory as already discussed by Fast et al. (2009). Fast et al. (2009) presented a detailed comparison of simulated non-volatile BBOA (generated with the same inventory used here) with the same set of AMS observations, and have found similar BBOA underprediction at T0.

At the T1 site (Fig. 3b), similar difficulties are encountered. Predictions of both model simulations are substantially below the observed levels with an underprediction of ~70% of observed BBOA, largely associated with the early morning discrepancies. A somewhat better agreement is reached in the late afternoon.

3.2.2 Secondary organic aerosols

We next examine the model skill in predicting secondary organic aerosols at the surface and the role of S/IVOC vapors in the formation of SOA. According to our earlier study (Hodzic et al., 2009) SOA production from anthropogenic and biogenic precursors based on the traditional modeling approach could explain less than 35% (see Table 2) of OOA within the city during the MILAGRO experiment (15% attributed to anthropogenic precursors). The comparison of observed and predicted SOA time series shown in Figs. 2c and 3c suggest a substantial enhancement in SOA concentrations at both urban and suburban locations when SI-SOA is taken into account.

At T0 (Fig. 2c), the ROB simulation captures the overall magnitude of observations reasonably well with an increase in average modeled SOA from 2.6 $\mu g/m^3$ (REF simulation) to 6.2 $\mu g/m^3$ for ROB which is in a better agreement with the observed value of 7.9 $\mu g/m^3$ (Table 2). The increase in correlation coefficient from 0.37 to 0.45 also denotes a more consistent temporal agreement between model and observations. The

ROB model captures within a factor of two the photochemical production of SOA in the late morning (~09:00–11:00 a.m. LT) and the production is maintained despite the growth of the convective boundary layer that was causing SOA to evaporate in the traditional model (Hodzic et al., 2009). If SI-SOA evaporation occurs in the ROB model during this photochemically active period, the vapors can be quickly oxidized and repartition to the particle phase (Dzepina et al., 2009). The predicted nighttime values are about 4 $\mu g/m^3$ and are consistent with OOA. The ROB model predicts somewhat lower production of SOA during the day near the source region leading to underpredicted SOA peak values, in particular after 24 March by a factor of 2. The passage of a cold surge led to precipitation on the 24 March and suppression of biomass burning, so that the underestimation by the ROB model stems directly from the representation of urban SOA production. At the T1 site, strong enhancement in predicted SOA concentrations is obtained with an increase in average levels from 1.1 $\mu g/m^3$ (REF simulation) to 4.4 $\mu g/m^3$ for the ROB simulation, leading to a fairly good agreement with observations particularly in terms of absolute values (the model bias ~8%).

The GRI parameterization tends to produce substantially higher SOA mass than ROB both in the immediate vicinity of sources and at the edge of the city. At the T0 site (Fig. 2c), a factor of two higher average SOA levels are computed (~12.2 $\mu g/m^3$). The late morning SOA enhancement (09:00–11:00 a.m. LT) reaches 12 $\mu g/m^3$ in the model which is 30% higher than observed (~9 $\mu g/m^3$). The model has the tendency to overpredict the observed levels on 16, 17, and 21 March, while a much better correspondence with OOA levels is achieved after 24 March. This overprediction coincides with periods of high atmospheric stability during which the wind speed was underpredicted in the model (and close to zero) leading to an unrealistic accumulation of pollutants during the day, which was also visible in predicted levels of CO (Hodzic et al., 2009).

A larger overprediction by the GRI model can be noted at the T1 site (Fig. 3c) almost everyday. The model predicts factor of two higher SOA levels. In particular, the photochemical production from 09:00 a.m.–01:00 p.m. LT is far larger than observed

(8 $\mu g/m^3$ for predicted SOA increase vs. 1 $\mu g/m^3$ increase for OOA). The correlation coefficient is also decreased in comparison to the ROB simulation. The results suggest that the updated treatment of S/IVOC aging used in the GRI model leads to unrealistically high SOA production downwind of the source region, consistent with the results of Dzepina et al. (2009). The likely reason for this enhancement in GRI SOA production in comparison to ROB is the addition of 40% oxygen in mass and the drop of two orders of magnitude in volatility upon each oxidation step (instead of 7.5%, and 1 order of magnitude for ROB) that facilitate the transfer to the aerosol phase. Our findings are consistent with results of a box model study of Dzepina et al. (2009) in which it was shown that the GRI approach leads to 62% higher SOA production compared to ROB.

3.2.3 Total organic aerosols

Comparisons of predicted total OA suggest that the implementation of the SI-SOA mechanisms improves model ability to predict SOA formation. At the urban T0 site (Fig. 2d), predicted TOA lies in the variability range associated with the observations: both ROB and GRI simulations show lower absolute bias (<25%) than the traditional simulation (~45%). No substantial improvement is however seen in simulated TOA temporal variability, which correlates slightly better for ROB (R^2=0.44) than for GRI (R^2=0.38) and is similar to REF (R^2=0.45). The fairly good agreement obtained for the GRI simulation is also partially due to error compensation between underpredicted POA concentrations in the morning and an overestimation of SOA production during that same period.

At the T1 site (Fig. 3d), the overprediction by GRI is obvious, with the bias in simulated TOA approaching 50%, and a drop in correlation coefficients down to 0.05. The excessive photochemical SI-SOA production in the early afternoon (12:00–15:00 p.m. LT) leads to almost a factor of 2 higher TOA levels than observed. The ROB predictions match the observed levels within 20%, although the temporal variability is not well captured (R^2=0.18). Similar to Hodzic et al. (2009), nighttime comparisons

appear more challenging at both sites as they are influenced by nighttime boundary layer effects, errors in the emissions or unaccounted oxidation processes.

3.2.4 Relative contributions to predicted SOA

The relative contribution of various sources to simulated SOA concentrations is shown in Fig. 4, including V-SOA from anthropogenic and biogenic precursors, and SI-SOA from anthropogenic and from biomass burning sources. For the ROB simulation, traditional and non-traditional precursors seem to equally contribute to the SOA budget in the source region (T0) during the 15–31 March period (Fig. 4a). During the day, about 2 $\mu g/m^3$ can be attributed to each anthropogenic and biogenic V-SOA, while about 4 $\mu g/m^3$ is due to anthropogenic SI-SOA and 1 $\mu g/m^3$ to biomass burning SI-SOA. The ratio of Ant. SI-SOA/V-SOA is similar to that found by Dzepina et al. (2009) and substantially higher than of Tsimpidi et al. (2009). The differences are probably explained by the fact that Tsimpidi et al. (2009) used very aggressive aging of V-SOA for which there is limited experimental evidence, but which greatly increases V-SOA formation. Such aging of V-SOA was not implemented here or by Dzepina et al. (2009). The relative contribution of SI-SOA increases substantially at the city edge (Fig. 4b) as vapors are continuously being oxidized and driven into the particle phase by the multigeneration oxidation mechanism. The anthropogenic SI-SOA stays elevated (i.e. close to 2.5 $\mu g/m^3$), and exceeds the anthropogenic V-SOA (<0.5 $\mu g/m^3$), or biogenic V-SOA (1.2 $\mu g/m^3$). SI-SOA from biomass burning contributes about 0.3 $\mu g/m^3$ throughout the day, which is of comparable magnitude to the contribution of anthropogenic V-SOA. A very different behavior is observed for the GRI simulation shown in Fig. 5, in which anthropogenic SI-SOA dominates the total SOA concentrations at both sites. Anthropogenic SI-SOA increase by 4–6 $\mu g/m^3$ at T0 (Fig. 5a) and 2–4 $\mu g/m^3$ at T1 (Fig. 5b) in comparison to the ROB simulation, while contributions of the other sources remain at similar levels.

3.3 O/C ratios

In addition to concentrations of organic aerosol species, AMS data provide the opportunity for evaluating the predicted oxygen to carbon (O/C) atomic ratio for the total OA. The measured O/C ratio of total OA is a good indicator of the level of processing and therefore the age of the organic aerosol (Aiken et al., 2008; DeCarlo et al., 2008; Jimenez et al., 2010; Ng et al., 2009; Heald et al., 2009). Typically, the values range from very low (<0.1) for e.g. vehicular emissions, to values close to 0.35–0.4 in freshly formed SOA, and up to 0.8–1 for aged air masses that contain more processed organic material. Therefore, the O/C ratio provides an additional constraint for evaluating SOA formation mechanisms. Model O/C ratios were estimated using measured chamber values for V-SOA (Ant V-SOA=0.37; Bio V-SOA=0.40), hydrocarbon-like organic aerosol (Ant POA=0.06), and biomass burning organic aerosol (BB POA=0.30) reported by Aiken et al. (2008) and Shiling et al. (2009). The organic carbon content in the secondary organic matter formed from the S/IVOC vapors was directly determined from modeled species as both carbon and oxygen fractions are explicitly modeled.

Figure 6a and b shows the spatial distribution of O/C ratio over the Mexico City region as predicted by the two SOA treatments. The lowest values are found in Mexico City and other smaller urban areas which are have a stronger influence of primary unprocessed organic material. The O/C increases progressively in the city outflow region as the POA gets diluted and as more SOA is formed with a higher contribution from higher generations of oxidation. The highest values are found in remote areas and are associated with the presence of aged background SOA. Although the spatial distribution is very similar for the two models, large differences exist in terms of absolute O/C ratio values. O/C average ratios ranging from 0.1 to 0.25 are found for ROB model over the Mexico City domain, while substantially higher average values are obtained for the GRI model ranging from 0.35 to 0.65. These later are in a better agreement with values reported by DeCarlo et al. (2008) for C-130 measurements that range from about 0.45 to 0.7 between the city and downwind areas.

This difference can also be seen in Fig. 6c that compares the simulated O/C values with estimated O/C values derived from AMS measurements at T0. The observed ratios range from 0.2 to 0.7 and display a strong diurnal amplitude with lower values in the morning (~06:00 a.m.) during the rush hour and in absence of photochemistry, and higher values during the day (~02:00–04:00 p.m.) when more secondary oxidized matter is being formed by photochemistry. The O/C ratios calculated from the ROB treatment are substantially lower than the observed levels, with values ranging from 0.08 in the morning to 0.2 in the early afternoon. The predicted SOA seems to be much less oxidized than the measured OOA, which is indicative of a too low addition of oxygen during oxidation in the ROB parameterization. A much better agreement with the observations is achieved for the GRI treatment in terms of magnitude and the temporal variability, although the predictions were consistently somewhat lower than observed after 24 March. The reason for this large difference between ROB and GRI models arises from the assumptions concerning the mass of oxygen that is added at each oxidation stage. Indeed, in ROB it is assumed that each generation of oxidation of S/IVOC vapors adds 7.5% to the mass of products due to the addition of oxygen atoms. This percentage is much larger for GRI, i.e. 40%. However the large addition of oxygen upon each oxidation step in the GRI parameterization has not been mechanistically explained. It is also possible that other mechanisms that are not considered in the present simulations, such as aerosol reactive uptake of very oxygenated such as glyoxal (Volkamer et al., 2007, 2009) is causing some of the rapid increase of oxygen in reality. Although the ROB treatment seems to perform better in terms of predicted surface concentrations, it results in far too low predicted O/C in OOA. This comparison show that the amount of oxygen in OA is an important constraint for determining the nature and the age of the aerosol, parameters that will play a key role in predicting the radiative forcing of organics in regional and climate models.

3.4 Evaluation of the SOA production aloft

3.4.1 Model evaluation along G-1 and C-130 flight paths

S/IVOC vapors can undergo several generations of oxidation and have the potential to continuously contribute to the production of SI-SOA further downwind of the city. AMS measurements from aboard the G-1 aircraft (Kleinman et al., 2008) and the C-130 aircraft (DeCarlo et al., 2008) during MILAGRO are available study the evolution and growth of organic aerosols aloft and downwind of Mexico City. Data from 8 G-1 flights are compared with the model outputs (including flights from 15a,b, 18a, 19a,b, 20a,b, 22a, where a and b refers to morning and afternoon flights). For the C-130, PMF-analyzed AMS data for only one flight (29 March) are available for comparison with the model. Figures 7 and 8 compare CO mixing ratios and organic aerosol species concentrations as predicted by ROB and GRI treatments and observed during two particular flights. It should be noted that G1 AMS data have been recently updated which resulted in a slightly different repartition between HOA and OOA aerosol components from the one reported in Fast et al. (2009) (based on 3-component PMF analysis). The updated data are used here. We also note that PMF performs better when using high-resolution AMS data instead of unit-resolution data, as the spectra of the different components are more distinct and easier to separate under high-resolution (DeCarlo et al., 2006; Aiken et al., 2009a).

On the morning flight of 19 March (Fig. 7), the aircraft arrived from the eastern part of the domain, crossed over the T1 site and performed a loop over Mexico City passing over T0 at 17:00–17:20 UTC, before sampling the outflow region north of the city around 18:00 UTC. As suggested by model OA predictions, the aircraft crossed several fire plumes that originated from the hills surrounding the city and were transported northward in the southerly flow. The comparison of observed and predicted CO mixing ratios shows the model skill in reproducing the magnitude and spatial variability observed in CO fields as indicated by a low overall bias (−50 ppbv) and the correlation coefficient (R^2) of 0.6. The highest concentrations are observed at 17:00 UTC over the

city with the predicted values close to 450 ppbv which is somewhat below the observed peak of 500 ppbv. This agreement for a chemically inert species such as CO indicates that the plume location and the transport of the pollutants are reasonably predicted on this particular day.

In contrast, modeling of OA appears to be more challenging and substantial differences can be seen between the ROB and GRI treatments. Although the observed total OA is reasonably well reproduced, with an overall underprediction of about 30% for the ROB simulation and no bias for the GRI simulation, the spatial variability is not well captured as indicated by low correlation coefficients (~0.22). The highest discrepancies are seen in the outflow region north of T1 (~17:50 UTC) and coincide with the underpredicted CO mixing ratios. This model error has likely a dynamic origin as explained by Fast et al. (2009). Relatively small errors in the wind speed and wind direction are likely to occur in this complex terrain as already reported in Fast et al. (2009) and Hodzic et al. (2009), and can cause plume misplacement of several km or the too rapid dispersion of the city plume. In terms of OA constituents, major inconsistencies are found for the BBOA fraction. Two out of four smoke plumes are either mislocated in the model or the amount of emitted smoke particles is highly overpredicted in the model estimates. The predicted smoke concentrations west of the T0 site and east of the T1 site both reach 4–6 $\mu g/m^3$ while these plumes are not reported in the observations. The comparison suggests that the plume along 98°40′ N is slightly shifted towards east and that concentrations in the plume center are lower. This inconsistency in BBOA predictions was also seen by Fast et al. (2009) that reported smoke concentrations above 15 $\mu g/m^3$ in the WRF/Chem model. It is likely the result of an inaccurate representation of the fire emissions (e.g. fuel types and consumption rates, flaming vs. smoldering regimes, etc.) which is not well represented in current fire emission inventories. Also, at this stage, rotational ambiguity in the unit mass resolution PMF results for BBOA and HOA cannot be discounted.

In addition, the modeled anthropogenic POA fraction for both the ROB and GRI simulations appears to be substantially lower than the observed HOA. The predicted av-

erage POA values (~0.3 $\mu g/m^3$) only account for about 30% of the observed HOA (~0.9 $\mu g/m^3$). This model underprediction seems equally important within the city boundary layer and in the downwind region. In comparison with the REF case, the model bias is increased from −0.1 to −0.6 $\mu g/m^3$ when the dynamic POA partitioning is considered. As already discussed in Sect. 3.2, the comparison with observations suggests that atmospheric HOA is less volatile than what is being assumed in the ROB and GRI approaches. It is likely that the simulated POA evaporates too steadily upon dilution of the urban plume in the growing PBL. Once evaporated, the primary organic vapors are oxidized into less volatile species that are likely to re-condense and form SOA. It should also be mentioned that our results for the REF case (POA considered as inert) show a better agreement with observations than the ones reported by Fast et al. (2009) due to changes in HOA estimates in the more recent PMF results. According to their comparison results, a large model POA underprediction was a common feature to all G1 flights, and the underprediction could reach up to a factor of 4 (i.e. the morning flight of 18 March). In our study the POA underprediction occurs but is generally more moderate.

Interestingly the best agreement is found for the predicted secondary organic fraction, with a good correspondence with OOA over the city as well as north of T1. Both ROB and GRI treatments are somewhat lower in terms of average predicted levels with a negative bias of 0.9 and 0.3 $\mu g/m^3$, respectively for the observed average OOA of ~2.8 $\mu g/m^3$. Similar to POA particles, the dilution of the plume also has a tendency to evaporate the freshly formed SOA. However this evaporation competes with the continuous formation of the new SOA downwind leading to a net production of the SOA mass as reported by Kleinman et al. (2008). The SOA concentrations predicted by the traditional SOA treatment are also displayed in Fig. 7 as a blue line. It can be clearly seen that the SOA production aloft over the city and downwind is insufficient when only traditional mostly aromatic precursors are considered, and is much improved when SI-SOA is added.

Another flight of interest to analyze SOA formation took place in the afternoon on

20 March. The airplane sampled exclusively the city outflow region as shown in Fig. 8, with three consecutive passes over the T1 site between 21:00 and 21:30 UTC and three passes north of T1 (the T2 site not shown here). Model simulations suggest the presence of a long narrow plume transported north of the city in the southwesterly flow. The outflow appears to be a mixture of the anthropogenic pollution originated from the city and the biomass burning emissions that took place on the hills southwest of T0. The six consecutive airplane encounters with the plume can clearly be identified in observed and predicted CO mixing ratios. The model was able to approximately predict the locations and absolute enhancements of the CO levels associated with the main plume most of the time, as well as the background levels of CO. The first and the last airplane overpasses were however performed at higher altitudes (between 4.5 and 5 km above ground level vs. 3–4 km for other periods) and suggest the model underprediction of the vertical extent of the plume. Concentrations at these higher altitudes are more challenging to simulate accurately due to the coarser model resolution at higher altitudes. In addition, the spatial structure of the plume is not well captured north of T1. A relatively small misplacement of the plume toward west can be seen, and is responsible for a reduced correlation with the observations (∼0.42) during this flight. Similar to CO mixing ratios, the predicted OA concentrations match reasonably well the observed levels within the plume, except for the elevated air mass at 21:00 UTC. The transition between elevated OA levels of 6–8 $\mu g/m^3$ found within the plume and the background concentrations of a few $\mu g/m^3$ seems well reproduced in the model. Up to 1.5 $\mu g/m^3$ higher OA levels are predicted with the GRI model compared to the ROB one.

The comparison of individual OA components suggests the occurrence of error compensation between a high SOA production, and low levels of anthropogenic POA. In particular, the SOA production from the GRI treatment is above (∼1 $\mu g/m^3$) OOA concentrations within the plume. However, the overall average OOA concentrations are captured well as suggested by relatively low bias (<50%) for both simulations. Comparing these SOA predictions from the traditional treatment shows that the S/IVOC chem-

istry is responsible for this increased agreement with the observations. On the other hand, the magnitude of the predicted anthropogenic POA is substantially lower than the observed HOA within the plume for both simulations, although somewhat higher concentrations are simulated inside the plume. Discrepancies can also be seen between simulated and observed BBOA, with more pronounced gradients in the model between the plume area (0.4 to 1.6 $\mu g/m^3$) and the remote background area that is not influenced by smoke. The observed BBOA levels show more uniform spatial structures, with higher background levels i.e. 0.4–0.6, indicating that greater dispersion of the smoke plume during this day than simulated by the model. It should be noted that our model results for primary organic aerosols generated from both anthropogenic and biomass burning sources agree well with WRF/Chem analysis of primary aerosol compounds reported by Fast et al. (2009).

A relatively similar model behavior with respect to OA formation is found for the C130 flight of 29 March (Fig. 9). This day is characterized by more stable atmospheric conditions leading to a greater accumulation of pollutants within the city basin than observed for the previous two flights (19–20 March). The pollution plume is located slightly west and northwest of T0. Modeled concentrations display a fairly good spatial agreement with measurements along the aircraft track for all species (e.g. CO: R^2=0.86), with exception of BBOA. The observed magnitude and temporal variability in CO concentrations is captured remarkably well. The predicted SOA levels for both S/IVOC runs match within 50% the observed concentrations (5–12 $\mu g/m^3$) along the first aircraft leg (∼18:30–19:30 UTC) north of the city. High OOA levels found within the urban plume (∼15–20 $\mu g/m^3$) are reasonably reproduced by the GRI simulation, and within 30% for the ROB one. As for previous aircraft comparisons, the HOA levels are underpredicted by a factor of 2–3 by the model over the urban area, leading to an overall underprediction of observed OA concentrations reaching 50% for ROB and 30% for GRI, respectively.

Finally, scatter plots shown in Fig. 10 summarize the comparisons of observed and simulated organic aerosol concentrations for the ensemble of G-1 flights considered

in this study. The distinction is made between points measured aloft the MCMA area and in the remote regions. Most of the observed and simulated OA concentrations stay below 12 $\mu g/m^3$, and no systematic bias can be seen in model simulations. The higher OA levels (>12 $\mu g/m^3$) are observed over the city, but no clear difference in model performance can be noted between the city and the remote regions. The strong scatter around the 1:1 slope is likely associated with inaccuracies found in the predicted spatial features of the plume (i.e. plume extent and location), and therefore are related to dynamic processes rather than aerosol chemistry. To examine independently the SOA production in the plume from the transport (eliminate the sensitivity to the advection and mixing processes), in the next section we will consider the OA concentrations normalized to CO.

3.4.2 Continuous SOA growth in the aged plume

The comparison with aircraft data allows quantifying the changes in the OA concentrations as a function of photochemical age of the urban plume. Similar to Kleinman et al. (2008), the SOA production downwind of the city was estimated from the OA/ΔCO ratio (where ΔCO is CO minus its assumed 100 ppb background concentration) and the age of the plume was determined by $-\mathrm{Log}_{10}(\mathrm{NO_x}/\mathrm{NO_y})$. CO and organic aerosol concentrations display very different age dependencies. CO levels decrease as the urban plume is transported downwind of the emission sources upon dilution, tending towards the background levels. Chemically long-lived, CO can be considered as a reasonably conserved tracer for the urban emissions and their dispersion on shorter timescales. Conversely, OA concentrations decrease upon dilution at the same rate as CO, but also increase due to the continuous photochemical production of SOA. Therefore, concentrations of OA normalized to CO mixing ratios are a good indicator of the SOA growth as a function of the chemical age of the plume.

Figure 11a shows the OA/ΔCO ratio for Standard Pressure and Temperature (STP) conditions (273 K and 1 atm). STP conditions were used here to account for changes in OA concentrations due to changes in altitude of the airplane (i.e. changes in vol-

ume). Similar to Kleinman et al. (2008), comparison was performed only for aircraft points that satisfy the conditions summarized in Table 3. It can be seen that the observed OA/ΔCO ratio increases substantially as the plume ages as already observed in the outflow of several urban areas (de Gouw and Jimenez, 2010). The values increase from 20–30 $\mu g\,sm^{-3}\,ppm^{-1}$ in the fresh air mass up to 60–70 $\mu g\,sm^{-3}\,ppm^{-1}$ in a 1-day aged plume. Ratios predicted by the ROB treatment are in a reasonably good agreement with the observations, except for the very last point that seems overpredicted by nearly 30 $\mu g\,sm^{-3}\,ppm^{-1}$. The GRI treatment, however, overpredicts the OA growth rate (i.e. ∼30–40%) with values ranging from 20–40 $\mu g\,sm^{-3}\,ppm^{-1}$ to 80–100 $\mu g\,sm^{-3}\,ppm^{-1}$. This overprediction for the GRI treatment is consistent with the results already discussed at the surface.

OA/ΔCO ratios are, however, influenced by excessive model loss of POA by evaporation during the transport of the plume, and therefore it is difficult to appreciate the aerosol growth associated with the photochemistry. The comparison of OOA/ΔCO ratios reveals an excessive production of SOA downwind of the city mainly for the GRI parameterization as shown in Fig. 11b. The ROB simulation captures relatively well the SOA growth downwind of the city. The SOA/ΔCO ratios are in range 30–60 $\mu g\,sm^{-3}\,ppm^{-1}$ and 40–90 $\mu g\,sm^{-3}\,ppm^{-1}$ for ROB and GRI simulations, respectively, while the observed values suggest a more limited increase of 30–50 $\mu g\,sm^{-3}$ in SOA per ppm of CO in the 1/2-day to 1-day aged plume. The SOA growth from the updated GRI treatment is 40–50% higher on average mainly due to larger decrease of volatility and higher oxygen gain at each oxidation step of S/IVOC vapors. Similar values (∼62%) are reported by a box model study of Dzepina et al. (2009). This active production of SOA downwind of Mexico City contrast greatly with the severe underprediction of the SOA production simulated by the traditional SOA model (Hodzic et al., 2009) in which ΔSOA was below 20 $\mu g\,sm^{-3}\,ppm^{-1}$ and was mainly associated with the presence of biogenic background SOA concentrations.

4 Conclusions

In this study a meso-scale chemistry-transport model has been applied to investigate the role of semi-volatile and intermediate volatility primary organic vapors in the formation of SOA in the vicinity of Mexico City. Model results have been assessed against several sets of AMS measurements obtained at the surface within the city and aloft in the outflow region during the March 2006 MILAGRO field experiment. The model has been updated to account for the dynamic treatment of POA emissions which includes both the gas/particle partitioning of primary species and the photochemical processing of associated vapors. Two approaches based on Robinson et al. (2007) and Grieshop et al. (2009) have been applied and inter-compared. The following are the principal findings of this study:

1. Model results suggest that organic aerosol formation from primary organic vapors has the potential to increase SOA levels substantially both within Mexico City where POA emissions are the highest, and in the surrounding regions that are influenced by the transport and aging of S/IVOC vapors. The ROB and GRI parameterizations produce somewhat different SOA concentrations and properties due to differences in the assumptions associated with volatility, reaction rates and oxygen gain at each oxidation step.

2. In both treatments an enhancement in average SOA levels is predicted within the city in presence of S/IVOC (~3 $\mu g/m^3$ or a factor of 3 for ROB, and ~9 $\mu g/m^3$ or a factor of 6 for GRI) relative to the traditional mechanism, which substantially reduces the gap with OOA observations. For the ROB case, the predicted SOA lies slightly below OOA values but within 21% and 8% on average at the T0 and T1 sites, respectively. The diurnal profiles characterized by the rapid SOA increase after sunrise are well reproduced. Although the ROB case seems to capture relatively well the amount and the evolution of SOA in Mexico City, the predicted average O/C ratio of total OA is 3 times lower than the observed value. The updated GRI treatment produces a much better agreement for O/C ratios at the

surface in terms of their absolute values and temporal variability, but the SOA production is generally overestimated. The predicted SOA mass for the GRI case is higher compared to the OOA measurements, as indicated by an overprediction of 55% at T0 and 90% at T1.

3. Downwind SOA production persists actively due to continued photochemistry of multi-generation S/IVOC oxidation products. Similar to aircraft observations, the predicted OA/ΔCO ratio for the ROB case increases from 20–30 $\mu g\, sm^{-3}\, ppm^{-1}$ up to 60–70 $\mu g\, sm^{-3}\, ppm^{-1}$ between a fresh and 1-day aged air mass, while the GRI case produces a 20–30% higher OA growth than observed. Comparison with individual flights of 19, 20 and 29 March indicates a much improved prediction of SOA in comparison to the traditional approach (which was a factor of 5–10 too low) and an agreement generally within 30% with observations (see Fig. 12). This new framework proposed by Robinson et al. based on the volatility of primary organic species constitutes a considerable revision in our understanding of SOA formation and is likely to be one of the important SOA formation pathways.

4. The dynamic treatment of POA does not have major effects on its surface concentrations in the source region, and the model results remain close to ones obtained with the non-volatile POA assumption. However, both non-traditional treatments show a deficiency in regard to POA evolution with a tendency to over-evaporate POA upon dilution of the urban plume in the growing PBL and during the regional transport. Comparisons with measurements suggest that atmospheric HOA may be less volatile than assumed in these parameterizations.

5. This study highlights the important potential role of S/IVOC chemistry in the SOA budget in this region, and highlights the need for improvements in current parameterizations. Experimentally constrained amounts and partitioning/aging parameterizations of S/IVOC are urgently needed for further progress in this area. In particular, the effect of fragmentation of oxygenated species leading to higher volatility species (Kroll et al., 2009) needs to be taken into account. Parameter-

izations which explicitly track both volatility and oxidation state (e.g., Jimenez et al., 2010) may also allow improved predictions of OA evolution and aging.

Acknowledgements. The National Center for Atmospheric Research is operated by the University Corporation for Atmospheric Research on behalf of the National Science Foundation. We gratefully acknowledge N. Donahue (Carnegie Mellon University), A. Robinson (Carnegie Mellon University) and K. Dzepina (University of Colorado and NCAR) for valuable scientific discussions on this topic. JLJ was supported by NSF ATM-0449815 and NOAA OGP NA08OAR4310565. SM was supported in part by the US Department of Energy's Atmospheric Science Program (Office of Science, BER, Grant No. DE-FG02-ER63993).

References

Aiken, A. C., Salcedo, D., Cubison, M. J., Huffman, J. A., DeCarlo, P. F., Ulbrich, I. M., Docherty, K. S., Sueper, D., Kimmel, J. R., Worsnop, D. R., Trimborn, A., Northway, M., Stone, E. A., Schauer, J. J., Volkamer, R. M., Fortner, E., de Foy, B., Wang, J., Laskin, A., Shutthanandan, V., Zheng, J., Zhang, R., Gaffney, J., Marley, N. A., Paredes-Miranda, G., Arnott, W. P., Molina, L. T., Sosa, G., and Jimenez, J. L.: Mexico City aerosol analysis during MILAGRO using high resolution aerosol mass spectrometry at the urban supersite (T0) – Part 1: Fine particle composition and organic source apportionment, Atmos. Chem. Phys., 9, 6633–6653, 2009, http://www.atmos-chem-phys.net/9/6633/2009/.

Aiken, A. C., de Foy, B., Wiedinmyer, C., DeCarlo, P. F., Ulbrich, I. M., Wehrli, M. N., Szidat, S., Prevot, A. S. H., Noda, J., Wacker, L., Volkamer, R., Fortner, E., Wang, J., Laskin, A., Shutthanandan, V., Zheng, J., Zhang, R., Paredes-Miranda, G., Arnott, W. P., Molina, L. T., Sosa, G., Querol, X., and Jimenez, J. L.: Mexico City aerosol analysis during MILAGRO using high resolution aerosol mass spectrometry at the urban supersite (T0) – Part 2: Analysis of the biomass burning contribution and the modern carbon fraction, Atmos. Chem. Phys. Discuss., 9, 25915–25981, 2009, http://www.atmos-chem-phys-discuss.net/9/25915/2009/.

Aiken, A. C., DeCarlo, P. F., Kroll, J. H., Worsnop, D. R., Huffman, J. A., Docherty, K., Ulbrich, I. M., Mohr, C., Kimmel, J. R., Sueper, D., Zhang, Q., Sun, Y., Trimborn, A., Northway, M., Ziemann, P. J., Canagaratna, M. R., Onasch, T. B., Alfarra, R., Prevot, A. S. H., Dom-

men, J., Duplissy, J., Metzger, A., Baltensperger, U., and Jimenez, J. L.: O/C and OM/OC ratios of primary, secondary, and ambient organic aerosols with high resolution time-of-flight aerosol mass spectrometry, Environ. Sci. Technol., 42, 4478–4485, doi:10.1021/es703009q, 2008.

Bessagnet, B., Menut, L., Curci, G., Hodzic, A., et al.: Regional modeling of carbonaceous aerosol over Europe – Focus on Secondary Organic Aerosols, J. Atmos. Chem., 61(3), 175–202, 2009.

Capes, G., Murphy, J. G., Reeves, C. E., McQuaid, J. B., Hamilton, J. F., Hopkins, J. R., Crosier, J., Williams, P. I., and Coe, H.: Secondary organic aerosol from biogenic VOCs over West Africa during AMMA, Atmos. Chem. Phys., 9, 3841–3850, 2009, http://www.atmos-chem-phys.net/9/3841/2009/.

Chen, Q., Farmer, D. K., Schneider, J., et al.: Mass spectral characterization of submicron biogenic organic particles in the Amazon Basin, Geophys. Res. Lett., 36, L20806, doi:10.1029/2009GL039880, 2009.

DeCarlo, P. F., Kimmel, J. R., Trimborn, A., et al.: Field-deployable, high-resolution, time-of-flight aerosol mass spectrometer, Anal. Chem., 78, 8281–8289, 2006.

DeCarlo, P. F., Dunlea, E. J., Kimmel, J. R., Aiken, A. C., Sueper, D., Crounse, J., Wennberg, P. O., Emmons, L., Shinozuka, Y., Clarke, A., Zhou, J., Tomlinson, J., Collins, D. R., Knapp, D., Weinheimer, A. J., Montzka, D. D., Campos, T., and Jimenez, J. L.: Fast airborne aerosol size and chemistry measurements above Mexico City and Central Mexico during the MILAGRO campaign, Atmos. Chem. Phys., 8, 4027–4048, 2008, http://www.atmos-chem-phys.net/8/4027/2008/.

de Gouw, J. A., Middlebrook, A. M., Warneke, C., et al.: Budget of organic carbon in a polluted atmosphere: Results from the New England Air Quality Study in 2002, J. Geophys. Res., 110, D16305, doi:10.1029/2004JD005623, 2005.

de Gouw J. and Jimenez, J. L.: Organic aerosols in the earth's atmosphere, Environ. Sci. Technol., 43 (20), 7614–7618, 2009.

Donahue, N. M., Robinson, A. L., Stanier, C. O., and Pandis, S. N.: Coupled partitioning, dilution, and chemical aging of semivolatile organics, Environ. Sci. Technol., 40, 2635–2643, 2006.

Dzepina, K., Volkamer, R. M., Madronich, S., Tulet, P., Ulbrich, I. M., Zhang, Q., Cappa, C. D., Ziemann, P. J., and Jimenez, J. L.: Evaluation of recently-proposed secondary organic aerosol models for a case study in Mexico City, Atmos. Chem. Phys., 9, 5681–5709, 2009,

http://www.atmos-chem-phys.net/9/5681/2009/.
Emmons, L. K., Lamarque, J.-F., Hess, P. G., et al.: Impact of Mexico City emissions on regional air quality from MOZART-4 simulations, Atmos. Chem. Phys. Discuss., submitted, 2010.
Fast, J., Aiken, A. C., Allan, J., Alexander, L., Campos, T., Canagaratna, M. R., Chapman, E., DeCarlo, P. F., de Foy, B., Gaffney, J., de Gouw, J., Doran, J. C., Emmons, L., Hodzic, A., Herndon, S. C., Huey, G., Jayne, J. T., Jimenez, J. L., Kleinman, L., Kuster, W., Marley, N., Russell, L., Ochoa, C., Onasch, T. B., Pekour, M., Song, C., Ulbrich, I. M., Warneke, C., Welsh-Bon, D., Wiedinmyer, C., Worsnop, D. R., Yu, X.-Y., and Zaveri, R.: Evaluating simulated primary anthropogenic and biomass burning organic aerosols during MILAGRO: implications for assessing treatments of secondary organic aerosols, Atmos. Chem. Phys., 9, 6191–6215, 2009, http://www.atmos-chem-phys.net/9/6191/2009/.
Fraser, M. P., Cass, G. R., Simoneit, B. R. T., et al.: Air quality model evaluation data for organics. 5. C_6-C_{22} nonpolar and semipolar aromatic compounds, Environ. Sci. Technol., 32, 1760–1770, 1998.
Grieshop, A. P., Logue, J. M., Donahue, N. M., and Robinson, A. L.: Laboratory investigation of photochemical oxidation of organic aerosol from wood fires 1: measurement and simulation of organic aerosol evolution, Atmos. Chem. Phys., 9, 1263–1277, 2009, http://www.atmos-chem-phys.net/9/1263/2009/.
Hallquist, M., Wenger, J. C., Baltensperger, U., Rudich, Y., Simpson, D., Claeys, M., Dommen, J., Donahue, N. M., George, C., Goldstein, A. H., Hamilton, J. F., Herrmann, H., Hoffmann, T., Iinuma, Y., Jang, M., Jenkin, M. E., Jimenez, J. L., Kiendler-Scharr, A., Maenhaut, W., McFiggans, G., Mentel, Th. F., Monod, A., Prvt, A. S. H., Seinfeld, J. H., Surratt, J. D., Szmigielski, R., and Wildt, J.: The formation, properties and impact of secondary organic aerosol: current and emerging issues, Atmos. Chem. Phys., 9, 5155–5235, 2009, http://www.atmos-chem-phys.net/9/5155/2009/.
Heald, C. L., Jacob, D. J., Park, R. J., et al.: A large organic aerosol source in the free troposphere missing from current models, Geophys. Res. Lett., 32, L18809, doi:10.1029/2005GL023831, 2005.
Heald, C. L., Goldstein, A. H., Allan, J. D., Aiken, A. C., Apel, E., Atlas, E. L., Baker, A. K., Bates, T. S., Beyersdorf, A. J., Blake, D. R., Campos, T., Coe, H., Crounse, J. D., DeCarlo, P. F., de Gouw, J. A., Dunlea, E. J., Flocke, F. M., Fried, A., Goldan, P., Griffin, R. J., Herndon, S. C., Holloway, J. S., Holzinger, R., Jimenez, J. L., Junkermann, W., Kuster, W. C.,

Lewis, A. C., Meinardi, S., Millet, D. B., Onasch, T., Polidori, A., Quinn, P. K., Riemer, D. D., Roberts, J. M., Salcedo, D., Sive, B., Swanson, A. L., Talbot, R., Warneke, C., Weber, R. J., Weibring, P., Wennberg, P. O., Worsnop, D. R., Wittig, A. E., Zhang, R., Zheng, J., and Zheng, W.: Total observed organic carbon (TOOC) in the atmosphere: a synthesis of North American observations, Atmos. Chem. Phys., 8, 2007–2025, 2008, http://www.atmos-chem-phys.net/8/2007/2008/.
Heald, C. L., Kroll, J. H., Jimenez, J. L., Docherty, K. S., DeCarlo, P. F., Aiken, A. C., Chen, Q., Martin, S. T., Farmer, D. K., Artaxo, P., and Weinheimer, A. J.: A simplified description of organic aerosol composition and implications for atmospheric aging, Geophys. Res. Lett., submitted, 2009.
Hodzic, A., Jimenez, J. L., Madronich, S., Aiken, A. C., Bessagnet, B., Curci, G., Fast, J., Lamarque, J.-F., Onasch, T. B., Roux, G., Schauer, J. J., Stone, E. A., and Ulbrich, I. M.: Modeling organic aerosols during MILAGRO: importance of biogenic secondary organic aerosols, Atmos. Chem. Phys., 9, 6949–6981, 2009, http://www.atmos-chem-phys.net/9/6949/2009/.
Huffman, J. A., Ziemann, P. J., Jayne, J. T., Worsnop, D. R., and Jimenez, J. L.: Development and characterization of a fast-stepping/scanning thermodenuder for chemically-resolved aerosol volatility measurements, Aerosol Sci. Tech., 42, 395–407, 2008.
Huffman, J. A., Docherty, K. S., Aiken, A. C., Cubison, M. J., Ulbrich, I. M., DeCarlo, P. F., Sueper, D., Jayne, J. T., Worsnop, D. R., Ziemann, P. J., and Jimenez, J. L.: Chemically-resolved aerosol volatility measurements from two megacity field studies, Atmos. Chem. Phys., 9, 7161–7182, 2009, http://www.atmos-chem-phys.net/9/7161/2009/.
Huffman, J. A., Docherty, K. S., Mohr, C., et al.: Chemically-resolved volatility measurements of organic aerosol from different sources, Environ. Sci. Technol., 43, 5351–5357, doi:10.1021/es803539d, 2009.
Jimenez, J. L., Canagaratna, M. R., and Donahue, N. M.: Evolution of organic aerosols in the atmosphere, Science, 326(5959), 1525–1529, 2009.
Kanakidou, M., Seinfeld, J. H., Pandis, S. N., Barnes, I., Dentener, F. J., Facchini, M. C., Van Dingenen, R., Ervens, B., Nenes, A., Nielsen, C. J., Swietlicki, E., Putaud, J. P., Balkanski, Y., Fuzzi, S., Horth, J., Moortgat, G. K., Winterhalter, R., Myhre, C. E. L., Tsigaridis, K., Vignati, E., Stephanou, E. G., and Wilson, J.: Organic aerosol and global climate modelling: a review, Atmos. Chem. Phys., 5, 1053–1123, 2005, http://www.atmos-chem-phys.net/5/1053/2005/.
Kleinman, L. I., Springston, S. R., Daum, P. H., Lee, Y.-N., Nunnermacker, L. J., Senum, G. I., Wang, J., Weinstein-Lloyd, J., Alexander, M. L., Hubbe, J., Ortega, J., Canagaratna, M.

R., and Jayne, J.: The time evolution of aerosol composition over the Mexico City plateau, Atmos. Chem. Phys., 8, 1559–1575, 2008, http://www.atmos-chem-phys.net/8/1559/2008/.

Kroll, J. H., Smith, J. D., Che, D. L., Kessler, S. H., Worsnop, D. R., and Wilson, K. R.: Measurement of fragmentation and functionalization pathways in the heterogeneous oxidation of oxidized organic aerosol, Phys. Chem. Chem. Phys., 11, 8005–8014, doi:10.1039/b905289e, 2009.

Lipsky, E. M. and Robinson, A. L.: Effects of dilution on fine particle mass and partitioning of semivolatile organics in diesel exhaust and wood smoke, Environ. Sci. Technol., 40, 155–162, 2006.

Murphy, D. M., Cziczo, D. J., Froyd, K. D., Hudson, P. K., Matthew, B. M., Middlebrook, A. M., Peltier, R. E., Sullivan, A., Thomson, D. S., and Weber, R. J.: Single-particle mass spectrometry of tropospheric aerosol particles, J. Geophys. Res., 111, D23S32, doi:10.1029/2006JD007340, 2006.

Murphy, B. N. and Pandis, S. N.: Simulating the formation of semivolatile primary and secondary organic aerosol in a regional chemical transport model, Environ. Sci. Technol., 43, 4722–4728, 2009.

Ng, N. L., Canagaratna, M. R., Zhang, Q., Jimenez, J. L., Tian, J., Ulbrich, I. M., Kroll, J. H., Docherty, K. S., Chhabra, P. S., Bahreini, R., Murphy, S. M., Seinfeld, J. H., Hildebrandt, L., DeCarlo, P. F., Lanz, V. A., Prevot, A. S. H., Dinar, E., Rudich, Y., and Worsnop, D. R.: Organic aerosol components observed in worldwide datasets from aerosol mass spectrometry, Atmos. Chem. Phys. Discuss., 9, 27745–27789, 2009, http://www.atmos-chem-phys-discuss.net/9/27745/2009/.

Odum, J. R., Hoffmann, T., Bowman, F., Collins, D., Flagan, R. C., and Seinfeld, J. H.: Gas/particle partitioning and secondary organic aerosol yields, Environ. Sci. Technol., 30, 2584–2585, 1996.

Pankow, J. F.: An absorption model of gas/particle partitioning of organic compounds in the atmosphere, Atmos. Environ., 28, 1994.

Pun, B. K. and Seigneur, C.: Investigative modeling of new pathways for secondary organic aerosol formation, Atmos. Chem. Phys., 7, 2199–2216, 2007, http://www.atmos-chem-phys.net/7/2199/2007/.

Reid, J. S., Koppmann, R., Eck, T. F., and Eleuterio, D. P.: A review of biomass burning emissions part II: intensive physical properties of biomass burning particles, Atmos. Chem. Phys., 5, 799–825, 2005, http://www.atmos-chem-phys.net/5/799/2005/.

Robinson, A. L., Donahue, N. M., Shrivastava, M. K., Weitkamp, E. A., Sage, A. M., Grieshop, A. P., Lane, T. E., Pandis, S. N., and Pierce, J. R.: Rethinking organic aerosols: Semivolatile emissions and photochemical aging, Science 315, 1259–1262, 2007.

Sage, A. M., Weitkamp, E. A., Robinson, A. L., and Donahue, N. M.: Evolving mass spectra of the oxidized component of organic aerosol: results from aerosol mass spectrometer analyses of aged diesel emissions, Atmos. Chem. Phys., 8, 1139–1152, 2008, http://www.atmos-chem-phys.net/8/1139/2008/.

Sheehy, P. M., Volkamer, R., Molina, L. T., and Molina, M. J.: Oxidative capacity of the Mexico City atmosphere – Part 2: A RO_x radical cycling perspective, Atmos. Chem. Phys. Discuss., 8, 5359–5412, 2008, http://www.atmos-chem-phys-discuss.net/8/5359/2008/.

Shilling, J. E., Chen, Q., King, S. M., Rosenoern, T., Kroll, J. H., Worsnop, D. R., DeCarlo, P. F., Aiken, A. C., Sueper, D., Jimenez, J. L., and Martin, S. T.: Loading-dependent elemental composition of a-pinene SOA particles, Atmos. Chem. Phys., 9, 771–782, 2009, http://www.atmos-chem-phys.net/9/771/2009/.

Shrivastava, M. K., Lane, T. E., Donahue, N. M., Pandis, S. N., and Robinson, A. L.: Effects of gas particle partitioning and aging of primary emissions on urban and regional organic aerosol concentrations, J. Geophys. Res., 113, D18301, doi:10.1029/2007JD009735, 2008.

Simpson, D., Yttri, K. E., Klimont, Z., Kupiainen, K., Caseiro, A., Gelencsér, A., Pio, C., Puxbaum, H., and Legrand, M.: Modeling carbonaceous aerosol over Europe: analysis of the CARBOSOL and EMEP EC/OC campaigns, J. Geophys. Res., 112, D23S14, doi:10.1029/2006JD008158, 2007.

Slowik, J. G., Stroud, C., Bottenheim, J. W., Brickell, P. C., Chang, R. Y.-W., Liggio, J., Makar, P. A., Martin, R. V., Moran, M. D., Shantz, N. C., Sjostedt, S. J., van Donkelaar, A., Vlasenko, A., Wiebe, H. A., Xia, A. G., Zhang, J., Leaitch, W. R., and Abbatt, J. P. D.: Characterization of a large biogenic secondary organic aerosol event from eastern Canadian forests, Atmos. Chem. Phys. Discuss., 9, 18113–18158, 2009, http://www.atmos-chem-phys-discuss.net/9/18113/2009/.

Tsimpidi, A. P., Karydis, V. A., Zavala, M., Lei, W., Molina, L., Ulbrich, I. M., Jimenez, J. L., and Pandis, S. N.: Evaluation of the volatility basis-set approach for the simulation of organic aerosol formation in the Mexico City metropolitan area, Atmos. Chem. Phys. Discuss., 9, 13693–13737, 2009, http://www.atmos-chem-phys-discuss.net/9/13693/2009/.

Tunved, P., Hansson, H. C., Kerminen, V. M., Strom, J., Dal Maso, M., Lihavainen, H., Viisanen, Y., Aalto, P. P., Komppula, M., and Kulmala, M.: High natural aerosol loading over boreal

forests, Science, 312(5771), 261–263, 2006.

Ulbrich, I. M., Canagaratna, M. R., Zhang, Q., Worsnop, D. R., and Jimenez, J. L.: Interpretation of organic components from Positive Matrix Factorization of aerosol mass spectrometric data, Atmos. Chem. Phys., 9, 2891–2918, 2009, http://www.atmos-chem-phys.net/9/2891/2009/.

Volkamer, R., Jimenez, J. L., San Martini, F., Dzepina, K., Zhang, Q., Salcedo, D., Molina, L. T., Worsnop, D. R., and Molina, M. J.: Secondary organic aerosol formation from anthropogenic air pollution: rapid and higher than expected, Geophys. Res. Lett., 33, L17811, doi:10.1029/2006GL026899, 2006.

Volkamer, R., San Martini, F., Molina, L. T., et al.: A missing sink for gas-phase glyoxal in Mexico City: formation of secondary organic aerosol, Geophys. Res. Lett., 34, L19807, doi:10.1029/2007GL030752, 2007.

Volkamer, R., Ziemann, P. J., and Molina, M. J.: Secondary Organic Aerosol Formation from Acetylene (C_2H_2): seed effect on SOA yields due to organic photochemistry in the aerosol aqueous phase, Atmos. Chem. Phys., 9, 1907–1928, 2009, http://www.atmos-chem-phys.net/9/1907/2009/.

Yokelson, R. J., Crounse, J. D., DeCarlo, P. F., Karl, T., Urbanski, S., Atlas, E., Campos, T., Shinozuka, Y., Kapustin, V., Clarke, A. D., Weinheimer, A., Knapp, D. J., Montzka, D. D., Holloway, J., Weibring, P., Flocke, F., Zheng, W., Toohey, D., Wennberg, P. O., Wiedinmyer, C., Mauldin, L., Fried, A., Richter, D., Walega, J., Jimenez, J. L., Adachi, K., Buseck, P. R., Hall, S. R., and Shetter, R.: Emissions from biomass burning in the Yucatan, Atmos. Chem. Phys., 9, 5785–5812, 2009, http://www.atmos-chem-phys.net/9/5785/2009/.

Zavala, M., Herndon, S. C., Wood, E. C., Onasch, T. B., Knighton, W. B., Marr, L. C., Kolb, C. E., and Molina, L. T.: Evaluation of mobile emissions contributions to Mexico City's emissions inventory using on-road and cross-road emission measurements and ambient data, Atmos. Chem. Phys., 9, 6305–6317, 2009, http://www.atmos-chem-phys.net/9/6305/2009/.

Zhang, Q., Jimenez, J. L., Canagaratna, M. R., Allan, J. D., et al.: Ubiquity and dominance of oxygenated species in organic aerosols in anthropogenically-influenced Northern Hemisphere midlatitudes, Geophys. Res. Lett., 34, L13801, doi:10.1029/2007GL029979, 2007.

Table 1. Parameters used to compute the partitioning of semi-volatile primary organics.

C^* ($\mu g\,m^{-3}$) at 298 K	Robinson et al. (2007)[a]		Grieshop et al. (2009)[b]			
	POA volatility distribution (f_i) (%)	ΔH_{vap} ($kJ\,mol^{-1}$)	Molecular weight ($g\,mol^{-1}$)	f_i anthropogenic (%)	f_i wood-smoke (%)	ΔH_{vap} ($kJ\,mol^{-1}$)
0.01	3	112	524	3	0	77
0.1	6	106	479	6	0	73
1	9	100	434	9	10	69
10	14	94	389	14	14	65
10^2	18	88	344	18	33	61
10^3	30	82	299	30	33	57
10^4	40	76	254	40	10	54
10^5	50	70	208	50	0	50
10^6	80	64	163	80	0	46

[a] Molecular weight for all species for the ROB case is assumed to be 250 g/mol.

[b] The majority of intermediate volatile species (IVOC) is not accounted for in the traditional POA emission inventories. This additional contribution has been added here to $SVOC_7$, $SVOC_8$ and $SVOC_9$ and represent 1.5 times the mass reported in POA emissions as in Robinson et al. (2007).

Table 2. Comparison of observed and simulated OOA concentrations during the MILAGRO experiment for the (REF) reference model simulation with the SOA formation from traditional anthropogenic and biogenic VOC precursors (from Hodzic et al., 2009); and for two S/IVOC model simulations that in addition of traditional precursors includes also the semi-volatile primary organics following the approach of Robinson et al. (2007), or Grieshop et al. (2009).

OOA ($\mu g\,m^{-3}$)	Urban station (T0)			Suburban site (T1)		
	ROB	GRI	REF	ROB	GRI	REF
(*)Mean obs. ($\mu g\,m^{-3}$)	Observation: 7.90			Observation: 4.81		
Bias ($\mu g\,m^{-3}$)	−1.72	4.33	−4.91	−0.40	4.34	−3.51
RMSE ($\mu g\,m^{-3}$)	5.30	8.29	6.95	2.65	6.92	4.13
Correlation	0.45	0.56	0.37	0.27	0.20	0.18

(*)The bias is computed as follow: Bias($\mu g/m^3$)=$(1/N)\sum_i(M_i - O_i)$; the Root Mean Square Error is defined as: RMSE($\mu g/m^3$)=$\sqrt{(1/N)\sum_i(M_i - O_i)^2}$; where N is the number of samples, O_i are observations and M_i are model predictions. These indicators were computed on all OOA available data from the MILAGRO ground sites during March 2006.

(**)AMS measurements are compared with model predictions of both submicron SOA (<1.25 µm) and coarser SOA (<2.5 µm).

Table 3. Criteria that need to be satisfied for the comparisons of OA/CO ratios. This choice follows the recommendations of Kleinman et al. (2008).

Longitude	>98° W
CO	>100 ppb
CH_3CN	<0.2+0.4∗CO/1000
$(CO-100)/NO_y$	>15
$(CO-100)/NO_y$	<25
OA	$<50\,\mu g\,m^{-3}$
SO_2	<25 ppb

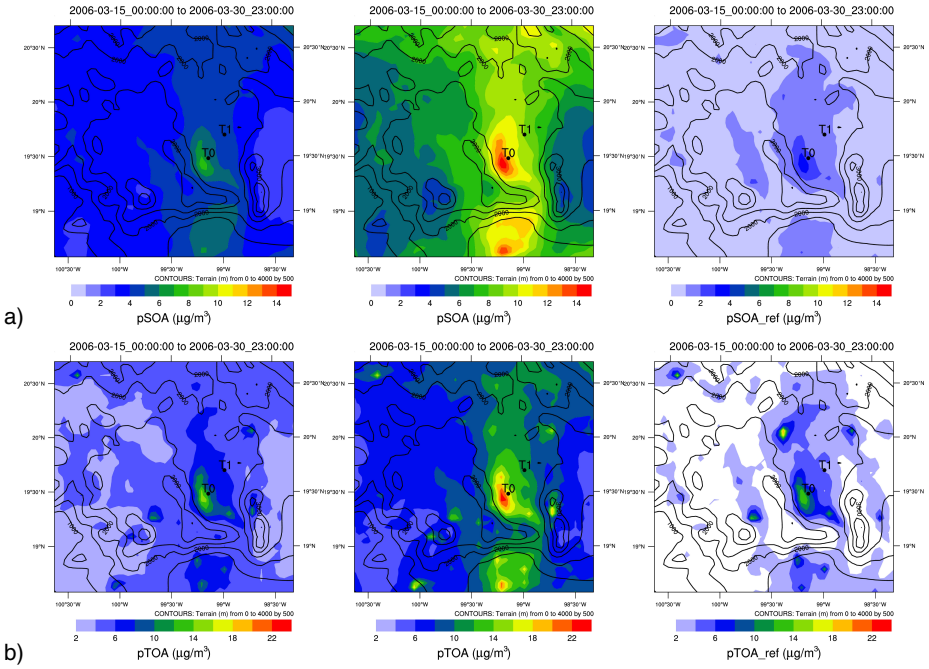

Fig. 1. Spatial distribution of secondary organic **(a)** and total organic **(b)** aerosols concentrations (µg/m^3) in $PM_{2.5}$ particles over the Mexico City basin as predicted by ROB (left panels), GRI (middle), and REF (right) simulations at the surface averaged between 15 and 31 March 2006.

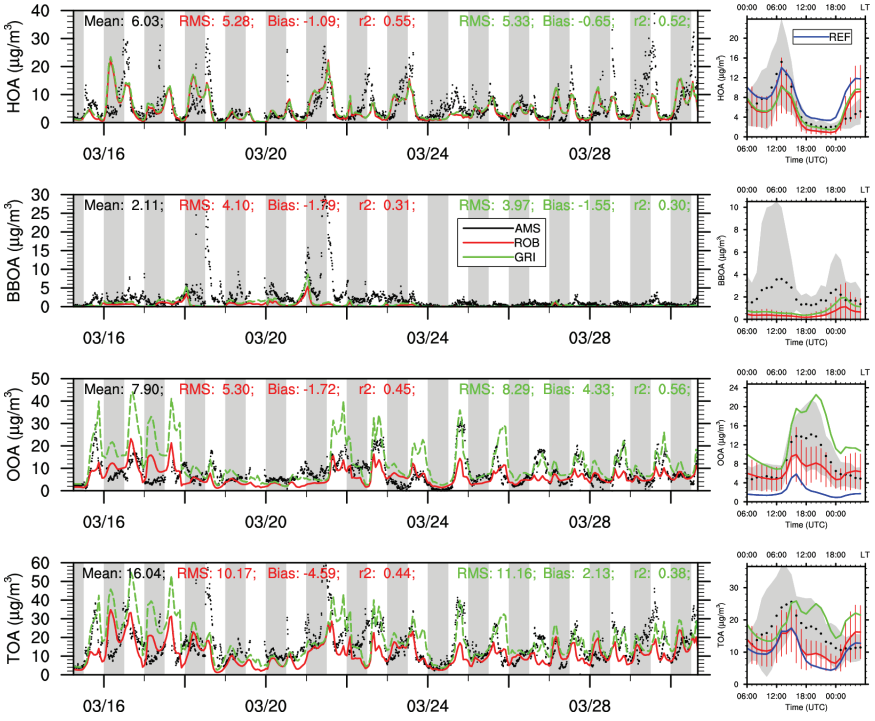

Fig. 2. Time series of modeled and observed surface concentrations of major carbonaceous aerosol compounds including primary organic aerosol from anthropogenic (HOA) and biomass burning emissions (BBOA), secondary organic matter (OOA), and total organic aerosols (TOA). Time series and average diurnal profile plots compare the ROB (red line) and GRI (green line) simulations, with the AMS measurements at T0 (given at ambient atmospheric conditions). The variability associated with average observations and model predictions is given in shaded area and red vertical bars, respectively, in the right panels. Diurnal profiles for the traditional simulation are also indicated for POA, SOA and TOA plots (blue line), where POA includes both anthropogenic and biomass burning contributions.

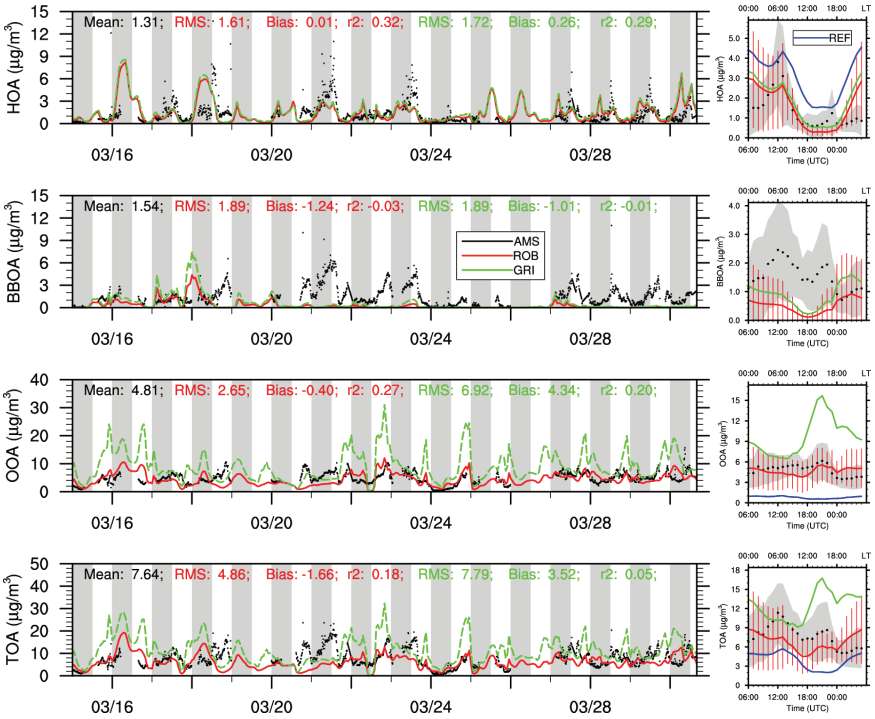

Fig. 3. Same as Fig. 2 except for the T1 site.

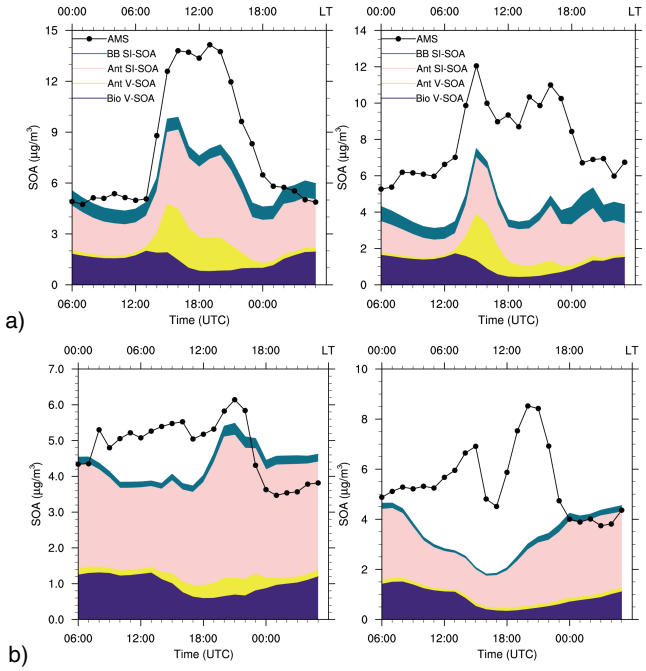

Fig. 4. Average diurnal profiles of oxygenated organic aerosol (OOA or SOA, µg/m^3) as observed and modeled (ROB run) during the 15–30 March comparison period (left panels) and the high biomass burning period (18–22 March, right panels) at **(a)** T0 and **(b)** T1. Black dots represent PMF values derived from AMS observations. Color polygons represent the contribution of each modeled SOA compound including SOA from biogenics (Bio V-SOA), traditional anthropogenics (Ant V-SOA), and non-traditional anthropogenics (Ant SI-SOA) and biomass burning (BB SI-SOA).

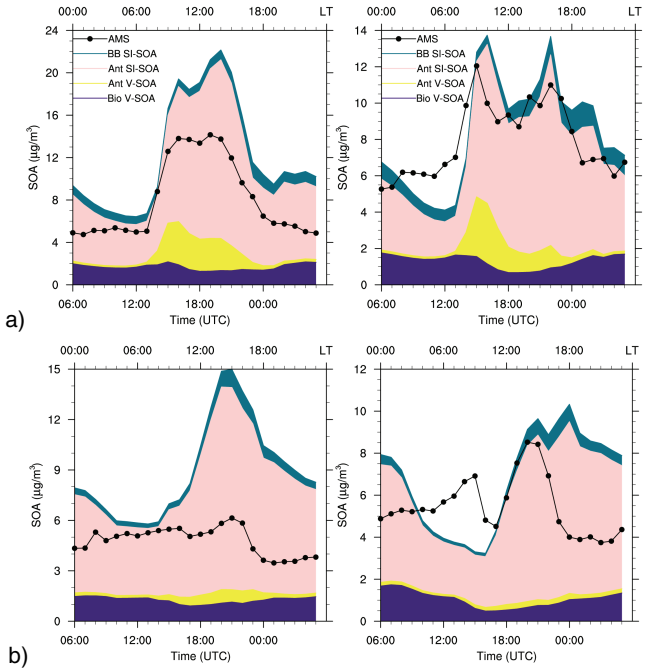

Fig. 5. Same as Fig. 4 but for GRI simulation.

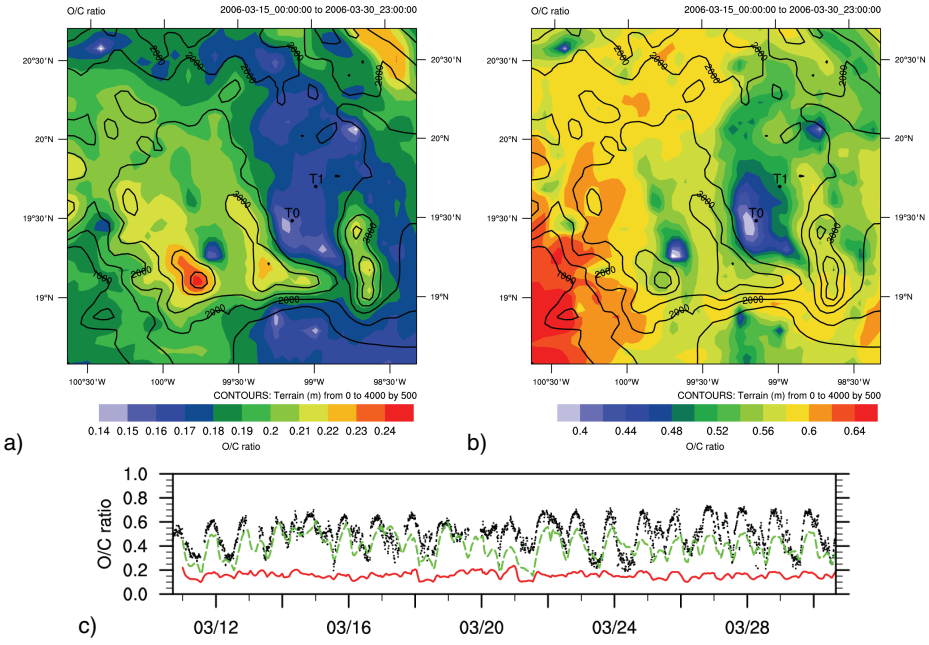

Fig. 6. Average mass O/C ratios over the Mexico City region as predicted by the ROB **(a)** and GRI **(b)** (treatments during the second half of March 2006. Values from the ROB (red line) and GRI (green line) simulations are also compared to AMS O/C retrievals (black dots) at T0 **(c)**.

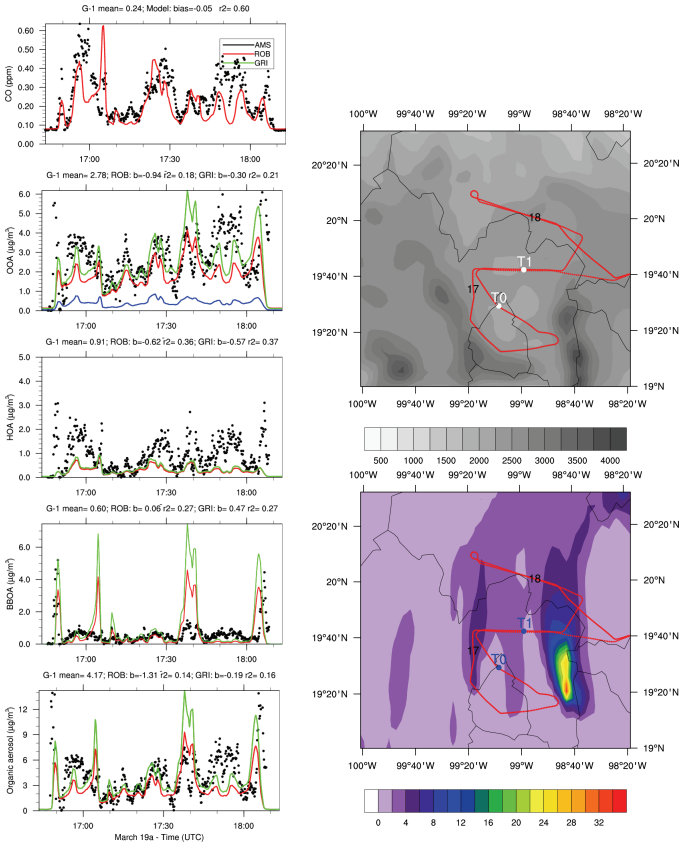

Fig. 7. Observed and predicted concentrations of CO, OOA, HOA, BBOA and total organic matter (μg/m^3) along the G1 flight path during 19 March 2006. Plots on the right indicate the location of G1 flight tracks and the simulated spatial extent of the OA plume (between 3–4 km of altitude).

705

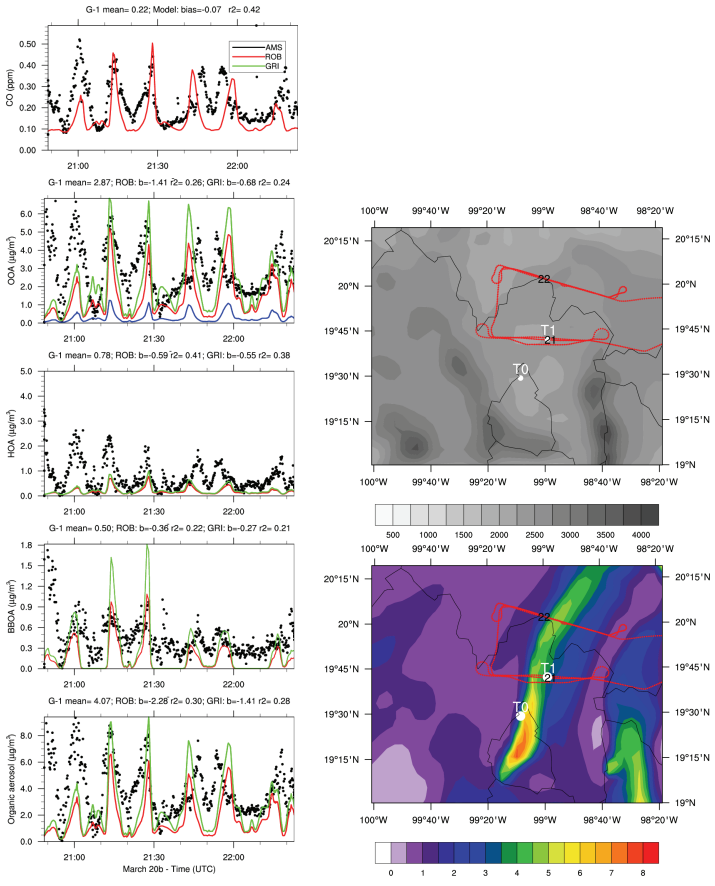

Fig. 8. Same as Fig. 7 except for the G1 flight of 20 March.

706

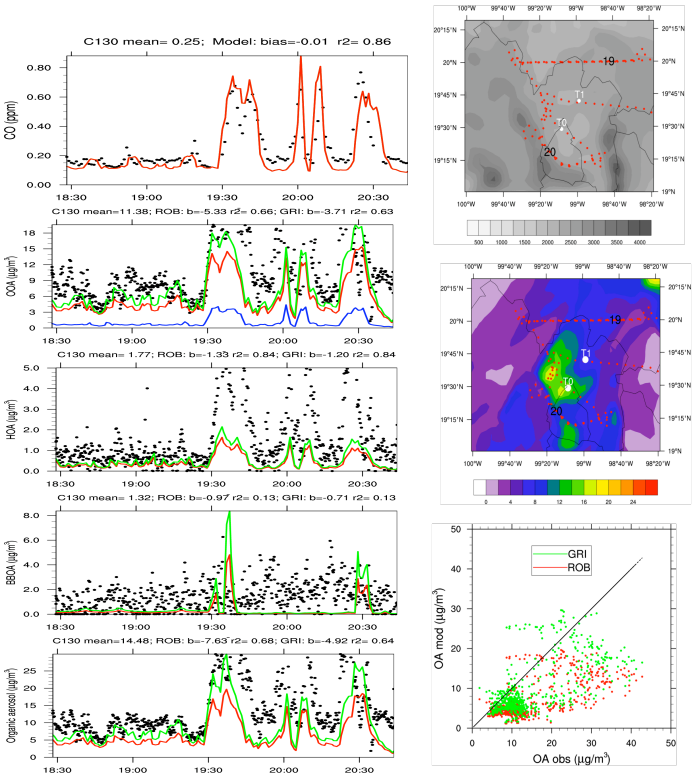

Fig. 9. Same as Fig. 7 except for the C130 flight of 29 March. Scatter plot comparing observed and predicted OA concentrations during this particular flight is shown for ROB (red dots) and GRI (green dots) simulations.

707

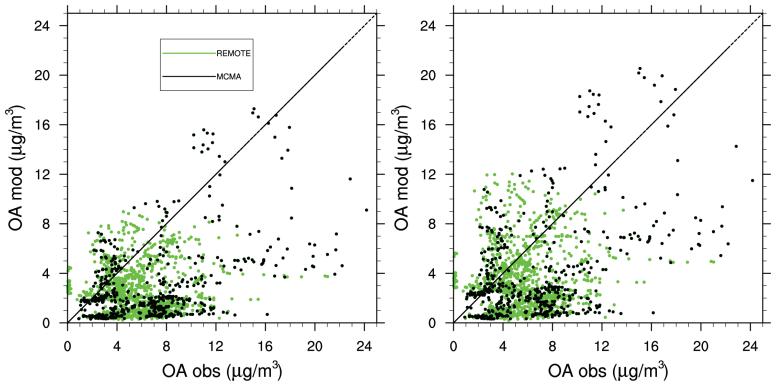

Fig. 10. Observed and predicted OA concentrations during eight MILAGRO G-1 flights in the vicinity of Mexico City. ROB (left panel) and GRI (right panel) simulations are shown. Comparison is restricted to points satisfying selection criteria shown in Table 3. Black points denote the comparison over Mexico City, while green dots correspond to the remote areas.

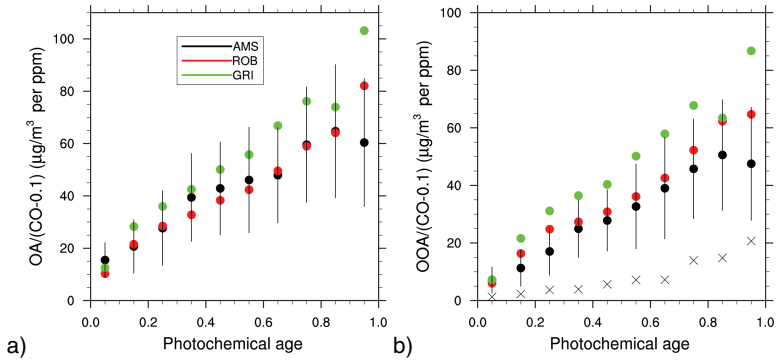

Fig. 11. OA **(a)** and OOA **(b)** concentration normalized to CO mixing ratios as a function of photochemical age. Model predictions for ROB (red) and GRI (green) runs are compared to AMS/PMF data collected aboard eight MILAGRO G-1 flights. Comparison is restricted to points satisfying selection criteria shown in Table 3. Concentrations are given at STP atmospheric conditions. Results for the traditional SOA simulation, denoted by black crosses, from Hodzic et al. (2009).

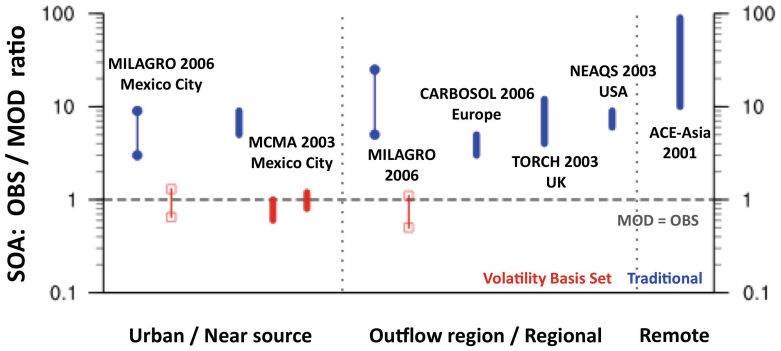

Fig. 12. Comparison of observed to predicted SOA ratios as determined in the present study (MILAGRO 2006) and reported in recent studies. MCMA 2003 summarizes results reported by Volkamer et al. (2006), Dzepina et al. (2009), and Tsimpidi et al. (2009); CARBOSOL 2006 refers to Simpson et al. (2007), TORCH 2003 refers to Johnson et al. (2006), NEAQS 2003 (de Gouw et al., 2005), ACD-Asia 2001 (Heald et al., 2005). In blue are represented estimates of the traditional SOA approach, while red refers to the volatility basis set.